Unravelling the DiscrepanciesDisparities in between Eulerian and Lagrangian Moisture Tracking Models in Monsoon- and Westerlies-dominated Basins Around of the Tibetan Plateau

Ying Li[1,2,3], Chenghao Wang[4,5], Qiuhong Tang[6], Shibo Yao[7], Bo Sun[8], Hui Peng[1], and Shangbin Xiao[1,2,3]

[1] College of Hydraulic and Environmental Engineering, China Three Gorges University, Yichang, China
[2] Engineering Research Center of Eco-environment in Three Gorges Reservoir Region, Yichang, China
[3] Three Gorges Reservoir Ecosystem Field Scientific Observation and Research Station, China Three Gorges University, Yichang, China
[4] School of Meteorology, University of Oklahoma, Norman, OK, USA
[5] Department of Geography and Environmental Sustainability, University of Oklahoma, Norman, OK, USA
[6] Key Laboratory of Water Cycle and Related Land Surface Processes, Institute of Geographic Sciences and Natural Resources Research, Chinese Academy of Sciences, Beijing, China
[7] China Meteorological Administration Key Laboratory for Climate Prediction Studies, National Climate Center, Beijing, China
[8] Collaborative Innovation Center on Forecast and Evaluation of Meteorological Disasters/Key Laboratory of Meteorological Disasters, Ministry of Education/Joint International Research Laboratory of Climate and Environment Change, Nanjing University of Information Science and Technology, Nanjing, China

Correspondence to: Ying Li (ly_hydro@outlook.com) and Shangbin Xiao (shangbinx@163.com)

Abstract. Eulerian and Lagrangian numerical moisture tracking models, which are which mainlyprimarily used to quantify moisture contributions from global sources to targetspecific regions from global sources, play a crucial role in hydrology and (paleo)climatology studies on the Tibetan Plateau (TP)Beyond traditional meteorological and (paleo)climatological analyses, numerical moisture tracking provides a quantitative diagnosis of moisture sources to the Tibetan Plateau (TP). However, with theDespite their widespread use of various numerical moisture tracking modelsapplications on the TP,While existing studies predominantly employ either the Eulerian or Lagrangian method, the potential differences discrepancies in their moisture tracking resultssimulations and their underlying causes of these discrepancies remain unexplored. In this study, we compare the applications of the most widely used Eulerian (WAM-2layers) and Lagrangian (FLEXPART-WaterSip) moisture tracking models in over the TP, i.e., WAM-2layers and FLEXPART-WaterSip, specifically focusing onin an Indian Summer Monsoon (ISM)-dominated basin (Yarlung Zangbo River Basin, YB) and a westerlies-dominated basin (upper Tarim River Basin, UTB). Compared to the bias-corrected FLEXPART-WaterSip, WAM-2layers model generally estimates higher moisture contributions from westerlies-dominated and distant source regions but lower contributions from local recycling. higher moisture contributions from westerlies-dominated and distant sources but lower contributions from local recycling and nearby sources opposite todownwind of the westerlies direction. However, WAM-2layers simulations tThese issuesdiscrepancies can be mitigated improved by using higherincreasing the spatial and temporal resolutions of forcing data in WAM-2layers. OneA notable advantage of WAM-2layers over FLEXPART-WaterSip is its closer alignment of that it simulates spatial

distribution ofestimated moisture sources with –moisture sources aligns more closely with the general pattern of actual evaporation, particularly in source regions characterized by alternatingwith complex land–sea distributions. HoweverIn additionHowever, the evaporation simulation biases ofin evaporation in FLEXPART-WaterSip can be partly corrected by athrough calibration process with actual surface fluxes. InFor moisture tracking over the TP, we recommend using for WAM-2layers application, we recommend selecting high-resolution forcing datasets with a focus on temporal resolution for WAM-2layers, while , prioritizing the temporal resolution; for FLEXPART-WaterSip application, we suggest applying bias corrections tobias-correcting the simulation results, including optimizee the filter offor precipitation particles and correctadjust the simulationevaporation biases of evaporationestimates.

The inherent ability in WAM-2layers to distinguish between evaporation and precipitation makes it more effectively in identifying varying moisture contributions arising from distinct surface evaporation sources. In contrast, in regions heavily influenced by smaller-scale convective systems with high spatial heterogeneity, such as the UTB when compared to the YB, simulations from FLEXPART-WaterSip tend to be more reliable. However, FLEXPART-WaterSip is prone to introducing additional errors when using specific humidity information in particles to infer moisture uptake and loss, although it accurately depicts the three-dimensional movement of air particles.

1 Introduction

Moisture tracking through numerical models play a pivotal role in advancing our quantitative understanding of the global and regional atmospheric water cycle, and is crucial for a variety of applications in meteorology, hydrology, and climate science (Gimeno et al., 2012; Gimeno et al., 2020). ~~Numerical models for moisture tracking can be broadly classified into two categories: Eulerian and Lagrangian methods. The Eulerian method generally employs a fixed spatial grid system with predefined grid spacing, and primarily focuses on averaged physical quantities over the atmospheric domain. Eulerian models simulate the movement and alteration of water vapor between adjacent grid cells by solving a system of water balance equations. Leveraging the discrete nature of grid cells to simplify numerical computations, they are well suited for describing large-scale hydrological circulations~~ (!!! INVALID CITATION !!! (van der Ent et al., 2014; Link et al., 2020))~~. In comparison, the Lagrangian method employs a particle trajectory tracking approach, inferring the movement of moisture through individual three-dimensional particle trajectories solved with differential equations. While Lagrangian models typically involves more complete physical mechanisms in particle dispersion processes, they exhibit substantially less numerical diffusion than Eulerian models, making them more adept at capturing small-scale atmospheric phenomena such as turbulence, convection, and dispersion, particularly over complex terrains~~ (!!! INVALID CITATION !!! (Wang et al., 2018; Tuinenburg and Staal, 2020))~~. To date, several studies have employed both types of models, such as Eulerian and Lagrangian approaches with COSMO model (Winschall et al., 2014), Eulerian and Lagrangian frameworks in "UTrack-atmospheric-moisture" (Tuinenburg and Staal, 2020) , and WRF-WVT and FLEXPART-WRF (Cloux et al., 2021), to diagnose regional moisture sources and have conducted comparative analyses. However, these studies have not extensively explored the limitations of different model types and the causes of discrepancies between moisture tracking results. Moreover, the studies on the generation mechanisms of model uncertainties through the moisture tracking intercomparison is severely lacking.~~

~~Encompassing the world's highest plateau, t~~The Tibetan Plateau (TP) region, often referred to as the "Asia water tower", encompasses the world's highest plateau and has been experiencing a rapid retreat of glaciers and permafrost, accompanied by shifts in precipitation patterns and a pronounced warming trend in recent decades (Yao et al., 2018; Yao et al., 2022). Numerous research efforts based on meteorological analyses and climate proxy indicators (e.g., precipitation and ice-core isotopes) have comprehensively investigated ~~into~~ the hydrologic~~al~~ cycle in this region ~~(Yao et al., 2013; Yang et al., 2014; Liu et al., 2020b),~~ (Yao et al., 2013; Yang et al., 2014; Liu et al., 2020b). ~~while r~~Recent advancements in numerical moisture tracking models have further facilitated the quantitative ~~analyses~~ diagnos~~e~~is of moisture source~~-~~-receptor relationships~~contribution~~ ~~to~~ ~~around~~across the TP region (Chen et al., 2012; Zhang et al., 2017; Li et al., 2022a). ~~To date~~In recent years, numerical moisture tracking has been widely used ~~for analysing~~to analyze precipitation and water resource changes over the TP (Li et al., 2019; Ayantobo et al., 2022; Zhang et al., 2023b), interpret~~ing~~ the ~~climatic background~~characteristics of TP's climate proxy indicators (Shao et al., 2021; Li et al., 2022b; Wang et al., 2022), and investigat~~ing~~e the impacts of TP's ~~hydrothermal~~ climatic conditions on downstream areas (Zhang et al., 2023a).

Table 1 We summarizesd the numerical moisture tracking studies over the TP infor the lpast twenty years (Table 1);, the utilized models can be Numerical models for moisture tracking can beand broadly classifiediedied the utilized models into two categories: Eulerian and Lagrangian frameworksmodels. The Eulerian moisture tracking approach typically methods(the Eulerian method generally employs a fixed spatial grid system and primarily focuses on averaged physical quantities overwith the predefined grid spacings, while the Lagrangian methodmodels employuses a particle tracking approach to infer, inferring the movement of moisture through individualdiagnosing source- receptor diagnosis)relationships. Among these models, Therein, the Water Accounting Model-2layers (WAM-2layers) and the FLEXible PARTicle dispersion model (FLEXPART) coupled with the “WaterSip” moisture source diagnostic method (FLEXPART-WaterSip) beingare the most widely use the predominant Eulerian and Lagrangian moisture tracking modelsmethod, respectively. Throughout As suggested in Table 1, The Eulerian method generally employs a fixed spatial grid system with predefined grid spacing, and primarily focuses on averaged physical quantities over the atmospheric domain. Eulerian models simulate the movement and alteration of water vapor between adjacent grid cells by solving a system of water balance equations. Leveraging the discrete nature of grid cells to simplify numerical computations, they are well suited for describing large-scale hydrological circulations (!!! INVALID CITATION !!! (van der Ent et al., 2014; Link et al., 2020)). In comparison, the Lagrangian method employs a particle trajectory tracking approach, inferring the movement of moisture through individual three-dimensional particle trajectories solved with differential equations. While Lagrangian models typically involves more complete physical mechanisms in particle dispersion processes, they exhibit substantially less numerical diffusion than Eulerian models, making them more adept at capturing small-scale atmospheric phenomena such as turbulence, convection, and dispersion, particularly over complex terrains (!!! INVALID CITATION !!! (Wang et al., 2018; Tuinenburg and Staal, 2020)). To date, several studies have employed both types of models, such as Eulerian and Lagrangian approaches with COSMO model (Winschall et al., 2014), Eulerian and Lagrangian frameworks in “UTrack-atmospheric-moisture” (Tuinenburg and Staal, 2020) , and WRF-WVT and FLEXPART-WRF (Cloux et al., 2021), to diagnose regional moisture sources and have conducted comparative analyses. However, these studies have not extensively explored the limitations of different model types and the causes of discrepancies between moisture tracking results. Moreover, the studies on the generation mechanisms of model uncertainties through the moisture tracking intercomparison is severely lacking.

We summarized the numerical moisture tracking studies over the TP in the last twenty years (Table 1), approximately one-fourth employed the Eulerian method, with the Water Accounting Model-2layers (WAM-2layers) being the predominant choice. The remaining three-fourths used the Lagrangian method, with the FLEXible PARTicle dispersion model (FLEXPART) and the “WaterSip” moisture source diagnostic method being the most widely applied. eExisting studies predominantly mainly used utilize a singular methodology (either Eulerian or Lagrangian method)moisture tracking models driven by very diverse forcing datasets, meanwhile covering various study periods and regions across, conducted over various study periods, across different regions in the TP, and with diverse forcing datasets. These diversitiesThis diversity largely hinders the quantitative comprehensive comparison of the moisture tracking results based fromon different models and the attribution of their

~~distinctions~~discrepancies. Nevertheless, ~~we~~ two general patterns can be observed through a quantitative comparison of the long-term moisture tracking results in these studies. ~~have examined figures presenting the long-term average spatial distributions of moisture sources in these studies.~~ First, ~~Some phenomena deserve our attention: 1) M~~moisture sources tracked by ~~the~~ Eulerian ~~method~~models tend to cover a large part of the western Eurasian continent and ~~could~~can -stretch southward to the southern Indian Ocean (Zhang et al., 2017; Li et al., 2019; Li et al., 2022a; Zhang et al., 2024)~~,~~. In contrast, ~~while~~ moisture sources tracked by ~~the~~ Lagrangian ~~method~~models predominantly extend southward (Chen et al., 2012; Sun and Wang, 2014; Chen et al., 2019; Yang et al., 2020), with broader westward extensions observed ~~limited to~~in the moisture tracking for the ~~most~~ westernmost TP and Xinjiang region (Zhou et al., 2019; Liu et al., 2020a; Yao et al., 2020; Hu et al., 2021). ~~2)~~ Second, ~~Generally,~~ areas with higher evaporation rates, such as the ~~water~~ocean surfaces, ~~tend to~~in general contribute more moisture compared to surrounding land areas. ~~As a result~~While~~,~~ the moisture sources simulated by Eulerian ~~method~~models aligns well with the land~~-~~–sea distribution (Zhang et al., 2017; Li et al., 2019; Li et al., 2022a; Zhang et al., 2024), ~~whereas~~ this ~~feature~~alignment is ~~not predominantly~~less pronounced ~~observed~~for ~~in the~~ Lagrangian ~~simulations~~models (Chen et al., 2012; Sun and Wang, 2014; Chen et al., 2019; Zhou et al., 2019; Liu et al., 2020a; Yang et al., 2020; Yao et al., 2020; Hu et al., 2021). In this context, we ~~have reason to~~ speculate that ~~the~~ different moisture tracking methods~~, particularly the~~ (both Eulerian ~~or~~and Lagrangian ~~method~~ones)~~s,~~ may involve certain unrecognized~~unnoticed errors/~~uncertainties or errors when applied to the TP region~~, urging us further exploration~~. This underscores the pressing need for further exploration to examine the discrepancies among these models to better characterize the complex hydrological processes of the T~~ibetan~~ P~~lateau~~.

Table 1: Overview of ~~Eulerian and Lagrangian~~ moisture tracking studies with Eulerian and Lagrangian models in the TP and its vicinity. Note that ~~there are~~ extensive studies on water isotopes in the TP ~~also encompass~~with moisture tracking simulations ~~to support their explanations~~ are included here ~~in the Table~~. "E and P" means the model diagnoses evaporation and precipitation separately, while "E – P" means the model diagnoses contributions through water budget (i.e., evaporation minus precipitation).

	Model	Moisture source diagnosis	Study area	Forcing dataset	Study period	Reference
Eulerian	WAM-1layer	E and P ~~–~~	Central-western TP	ERA-I, NCEP-2	1979–2013	Zhang et al. (2017)
	WAM-2layers	E and P ~~–~~	Endorheic TP	ERA-I, MERRA-2, JRA-55	1979–2015	Li et al. (2019)
	WAM-2layers	E and P ~~–~~	Southern/northern TP	ERA-I	1979–2016	Zhang et al. (2019a)
	WAM-2layers	E and P	TP	ERA-I	1979–2015	Guo et al. (2019)
	WAM-2layers	E and P	TP	ERA-I	1998–2018	Zhang (2020)
	WAM-2layers	E and P	TP	ERA-I, MetUM	1982–2012	Guo et al. (2019); Guo et al. (2020)
	WAM-2layers	E and P ~~–~~	Major basins in TP	ERA-I, MERRA-2, JRA-55	1979–2015	Li et al. (2022a)
	WAM-2layers	E and P	TP (forward tracking oceanic evaporation)	ERA-I, MERRA-2, JRA-55	1979–2015	Li et al. (2022b)
	WAM-2layers	E and P	TP (forward tracking TP evaporation)	ERA5	2000–2020	Zhang et al. (2023a)
	WAM-2layers	E and P	Five typical cells in the TP	ERA5	2011–2020	Zhang et al. (2024)

	CAM5.1 with a tagging method	E and P ~~–~~	Southern/northern TP	MERRA	1982–2014	Pan et al. (2018)
Lagrangian	FLEXPART	E – P	TP	NCEP-GFS	2005–2009 (summer)	Chen et al. (2012)
	FLEXPART	~~areal~~ Areal source–receptor attribution	Grassland on eastern TP	NCEP-CFSR	2000–2009	Sun and Wang (2014)
	FLEXPART	WaterSip	Four regions within TP	ERA-I	1979–2018 (May–August)	Chen et al. (2019)
	FLEXPART	~~areal~~ Areal source–receptor attribution	Xinjiang	NCEP-FNL	2008–2015 (April–September)	Zhou et al. (2019)
	FLEXPART	WaterSip	Southeastern TP	ERA-I	1980–2016 (June–September)	Yang et al. (2020)
	FLEXPART	WaterSip	Xinjiang	NCEP-CFSR	1979–2018	Yao et al. (2020)
	FLEXPART	WaterSip	Northern/Southern Xinjiang	NCEP-CFSR	1979–2018	Hu et al. (2021)
	FLEXPART	~~areal~~ Areal source–receptor attribution	Source region of Yellow River	NCEP-FNL	1979–2009	Liu et al. (2021)
	FLEXPART	WaterSip	Xinjiang	NCEP-CFSR	1979–2018 (April–September)	Yao et al. (2021)
	FLEXPART	E – P	Three-rivers headwater region	ERA-I	1980–2017 (boreal summer)	Zhao et al. (2021)
	FLEXPART	E – P	Three-rivers source region	NCEP-FNL	1989–2019	Liu et al. (2022)
	FLEXPART	WaterSip	Three-rivers headwater region	ERA-I	1980–2017	Zhao et al. (2023)
	HYSPLIT	WaterSip	Three-rivers headwater region	NNR1	1960–2017 (June–September)	Zhang et al. (2019b)
	HYSPLIT	E – P	Western TP	ERA-I	1979–2018 (winter)	Liu et al. (2020a)
	HYSPLIT	~~maximum~~ Maximum specific humidity	Seven regions within TP	NCEP/NCAR	1961–2015 (summer extreme event)	Ma et al. (2020)
	HYSPLIT	~~contribution~~ Contribution function and weighting	TP	NCEP-GDAS	1950–2015 (extreme precipitation events)	Ayantobo et al. (2022)
	HYSPLIT	WaterSip	Southern Xinjiang	ERA5	2021(June 15–17)	Chen et al. (2022)
	LAGRANTO	WaterSip	Southeastern TP	ERA-I	1979–2016 (winter extreme precipitation)	Huang et al. (2018)
	LAGRANTO	WaterSip	Three regions within TP	ERA-I	1979–2016 (winter extreme precipitation)	Qiu et al. (2019)
	LAGRANTO	WaterSip	Northern TP	ERA-I	2010–2018 (monsoon season)	Wang et al. (2023)
	QIBT	E and P	Southeastern TP	ERA-I	1982–2011 (April–September)	Xu and Gao (2019)

It is noteworthy that ~~Beyond the TP, s~~several studies have employed both ~~types of~~Eulerian and Lagrangian models to diagnose ~~regional~~ moisture sources and ~~have conducted~~perform comparative analyses in other regions. For example, a ~~a series of contrasts~~comparison among RCM-tag (~~build~~coupled with ~~in~~ MM5), WAM, and 3D-T (a modification of QIBT) models in West Africa revealed that the number of vertical layers and the mixing assumption ~~after~~for evaporation ~~have~~ significantly influence ~~on~~ simulations, especially in regions with strong wind shear (van der Ent et al., 2013). ~~The~~Another comparison between Eulerian and Lagrangian a~~(Winschall et al., 2014)~~pproaches (~~within~~implemented in the COSMO model) in Europe ~~indicated~~found that the linkage of moisture uptakes in the atmospheric boundary layer to evaporation in the Lagrangian ~~method~~approach ~~to link moisture uptakes in the atmospheric boundary layer to evaporation~~ is mostly consistent with the advanced ~~advanced~~ Eulerian ~~method~~model (Winschall et al., 2014). Tuinenburg and Staal (2020)~~Tuinenburg and Staal (2020)~~

compared a set of moisture tracking models for 7 source locations globally and concluded Under “UTrack-atmospheric-moisture” modelthat, the three-dimensional Lagrangian frameworkmodels were most accurate and considered more suitable for areas with relatively complex terrain, becauseas they can better describetrack moisture transport better under circumstances ofwith strong vertical variability in horizontal transport(Tuinenburg and Staal, 2020). TakingUsing the Eulerian WRF-WVT model as “ground trutha benchmark for moisture tracking over the Mediterranean region”, Cloux et al. (2021)Cloux et al. (2021) considered the Lagrangian model FLEXPART-WRF model was argued more appropriate for a qualitative description of moisture origin rather than a precise estimation of source contributions. sources a quantitative oneThe consensus among tThese comparative studies is to emphasize that the most suitable moisture tracking model depends on the specific case itself, such asincluding but not limited to the research question, the spatial extensiont, and the computing resource available. Despite the considerablethese existing effortsin other regions, it remains unclear whether their conclusions are applicable to moisture tracking the over the TP region. Moreover, the studies on the generation mechanisms of model uncertainties through moisture tracking intercomparison is still lackingfew studies have investigated the underlying mechanisms of the uncertainties and discrepancies observed among different modelsrelevant conclusions are challenging to apply universally to the TP environments, especially among the most commonly employed models in the TP. Moreover, the studies on the generation mechanisms of model uncertainties through the moisture tracking intercomparison is severely lacking on a global scale.

Our thorough review of the different studies in Table 1 indicates potential inherent differences, such as the range of moisture sources and capability to capture specific precipitation events, in the application of the two types of numerical moisture tracing models across the TP. This prompts the questions: what are the potential differences in moisture tracking when using these two types of models, and what are the causes of these differences?

The overall objective of In this study, we aim is to investigate potential errors/uncertainties in existing numerical moisture tracking models and the underlying mechanisms of their discrepancies research overon the TP. This is achieved and understand the underlying mechanisms contributing to these errors/uncertainties, through a comparison between thecompare the most commonly employed used Eulerian and Lagrangian moisture tracking models in the TP region, namely i.e.specifically WAM-2layers and FLEXPART-WaterSip (FLEXPART with “WaterSip” diagnostic method). Given that the TP's TP’s climate is predominantly mainly influenced shaped by the interactions between the Indian Summer Monsoon (ISM) and the mid-latitude westerlies, we have chosenselected two representative basin for our comparative analysis: an the ISM-dominated basin (the Yarlung Zangbo River Basin, (YB) and thea westerlies-dominated basin (the upper Tarim River Basin, (UTB) for our comparative analysis (Fig. S1 in the Supplement). Section 2 provides describes the mechanisms, forcing data, and numerical settings for both moisture tracking detailed information on the foundational mechanisms, input data, and settings of the two models. Section 3 offers provides a comprehensive comparison of the moisture tracking results simulations from the two models acrossfor both basins. Section 4 analyses delves into the intermediate processes involved inof moisture tracking in the two models, i.e.:, moisture fluxes in WAM-2layers and particle trajectories in FLEXPART. To further explore the inherentillustrate the differences between these two models, Section 5 specifieexamines the relationship between the simulated moisture contributions and actual evaporation from variousover the source regions. Section 6 introduces a two-step bias correction method for FLEXPART-WaterSip simulations~~,~~ based on a ~~the~~ comparison between actual and simulated surface fluxes. ~~Finally,~~ Section 7 further ~~Section 5 further~~ investigates the potential determinants of the observed ~~disparities~~ discrepancies between the two approaches~~models~~ through a series of carefully designed numerical experiments. ~~Overall, these comparisons and analyses are expected to serve as a reference for selecting and utilizing models, analyzing results, and correcting associated biases and errors in future studies on moisture tracking in the TP region.~~

2 Eulerian ~~(WAM-2layers)~~ and Lagrangian ~~(FLEXPART-WaterSip) methods~~approaches for moisture tracking: WAM-2layers and FLEXPART-WaterSip models

In this study, ~~T~~the WAM-2layers V3.0.0b5 is adopted for ~~the~~ Eulerian moisture tracking~~ in this study~~. ~~The~~ This two-layers version, ~~which is~~ designed to deal with ~~the~~ wind shear in the upper air, is an update to the ~~previously used~~earlier single-layer version (van der Ent et al., 2010). As illustrated in the conceptual ~~graphs~~ diagram (Fig. 1a), the underlying principle of WAM-2layers is the water balance equation (van der Ent et al., 2014), which in the lower layer is given by:

$$\frac{\partial S_{g,lower\cancel{k}}}{\partial t} = -\frac{\partial(S_{g,lower\cancel{k}}u)}{\partial x} \cancel{+} - \frac{\partial(S_{\cancel{k}g,lower}v)}{\partial y} + E_{\cancel{k}g} - P_{\cancel{k}g} \pm F_{v,g} \cancel{+ \xi_k} \quad (1)$$

~~Where~~ where subscript g denotes the tagged moisture; S is the moisture content in the atmosphere ~~S_k is the atmospheric moisture content in layer k~~; t is time; u and v are the zonal (x) and meridional (y) wind fields, respectively ~~in zonal (x) and meridional (y) directions~~; E is evaporation (which only occurs in the bottom layer); ~~and~~ P ~~are evaporation (occurs only in the bottom layer) and~~is precipitation; and F_v is the vertical moisture transport between the two layers~~; and ξ is the residual term~~. The model prescribes a two-layer structure, typically dividing at approximately ~~division (~~~810 hPa with a standard surface pressure~~)~~. ~~and m~~Modifi~~es~~cations to F_v (~~with~~ $4F_v$ in the net flux direction and $3F_v$ in the opposite direction) are implemented to ~~consider~~ account for turbulent moisture exchange. Note that the division between two layers varies with topography, ~~and it~~which decreases to ~520 hPa over ~~a~~the TP (~4000 m) ~~4000m altitude~~.

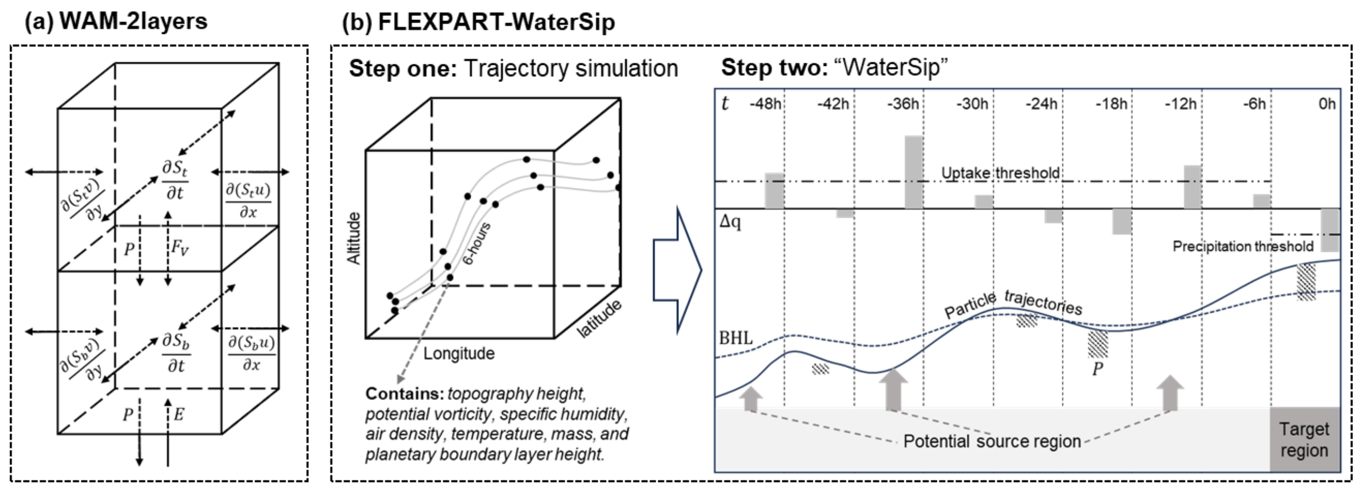

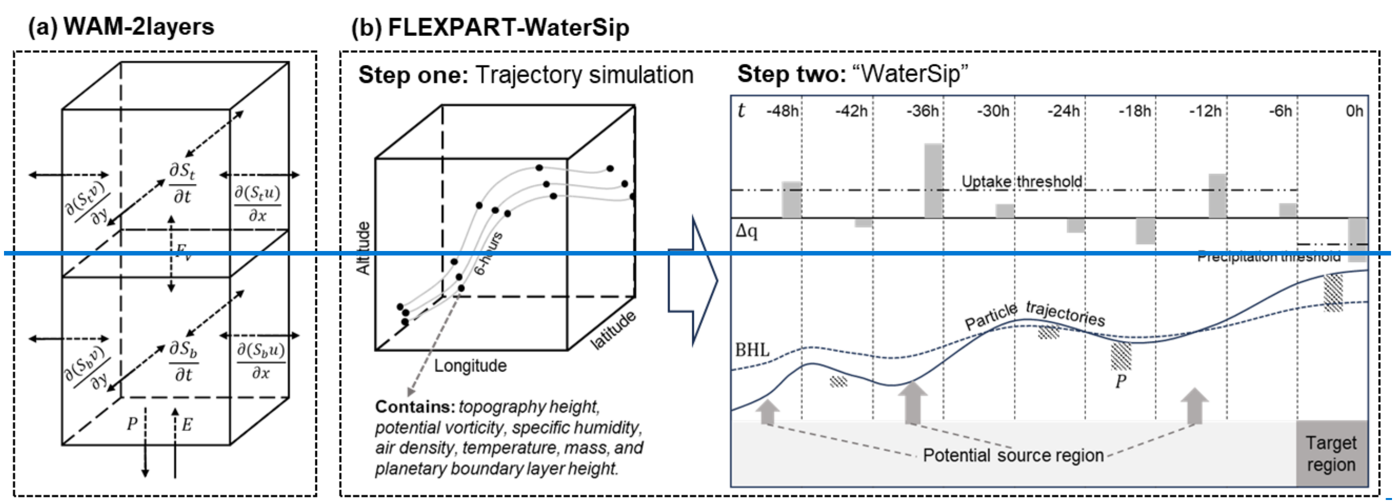

Figure 1: Mechanisms of (a) WAM-2layers ~~(a)~~ and (b) FLEXPART-WaterSip ~~(b) method~~models. "Step two" in (b) is adapted from Sodemann et al. (2008).

The Lagrangian particle trajectory simulation in this study is ~~implemented~~ conducted using FLEXPART V10.4, a versatile model widely employed to simulate the transport and turbulent mixing of gases and aerosols in the atmosphere (Pisso et al., 2019). FLEXPART can operates in~~The~~ domain-filling mode to represent the entire atmosphere ~~in FLEXPART adopts~~ using ~~evenly~~ uniformly distributed particles with equal mass.~~ to represent the entire atmosphere,~~ It is independent of a computational grid, which enables effective descriptions of atmospheric transport ~~offers a precise means to describe the global and regional atmospheric cycle~~ at a theoretically infinitesimal spatial ~~scale~~resolution. For~~In~~ this study, five million particles were released ~~from~~ at altitudes ranging from 100 m to 20,000 m across the entire ~~study~~ target region. The ~~domain-filling~~model outputs from FLEXPART include~~s~~ detailed three-dimensional position, topography height, potential vorticity, specific humidity, air density, temperature, mass, and planetary boundary layer height (BLH) of each particle/parcel at 6-hourly intervals (Fig. 1b). Similar to other Lagrangian models ~~like~~ such as HYSPLIT (Stein et al., 2016) and Lagranto (Sprenger and Wernli, 2015), FLEXPART on its own ~~cannot~~ does not identify potential moisture sources for precipitation in the target region nor quantify their contributions. To address this limitation, we adopted the "WaterSip" method proposed by Sodemann et al. (2008)~~ was adopted to identify potential moisture sources of the targeted moisture~~., This method identify moisture sources ~~mainly~~ using humidity information along ~~the~~ particle trajectories simulated by FLEXPART, which~~. This method~~ involves ~~critical~~ key ~~processing~~ processes ~~procedures (Fig. 1b)~~ such as filtering trajectories that lead to precipitation, calculating specific humidity changes and their attributed fractions, and determining potential moisture sources based on moisture uptake thresholds ~~as well as~~and BLH (Fig. 1b). A more detailed ~~methodology~~ description of this method can be found in Sodemann et al. (2008).~~ In this study, the d~~Default screening thresholds in this study are set at 0.2 g kg^{-1} for specific humidity change, 80% for relative humidity, and 1.5 times the BLH for particle height~~ are set at 0.2 g/kg, 80%, and 1.5 times BLH, respectively~~, although adjustments were made ~~. However, these threshold settings will be adjusted in the~~for sensitivity experiments detailed in Sections 6 and 7. In summary, the ~~the~~ FLEXPART-WaterSip ~~moisture tracking methodmodel~~approach adopted here~~ in this study~~ ~~intergrates~~integrates ~~both~~ the particle trajectory ~~simulation~~ simulated~~using~~ by FLEXPART ~~and~~ with the moisture source–receptor diagnostics ~~procedure using~~of "WaterSip".

Both WAM-2layers and FLEXPART-WaterSip ~~are~~ operate as offline models that rely on meteorological fields as forcing inputs. Here we used ~~T~~the fifth-generation atmospheric reanalysis product from the European Centre for Medium-Range Weather Forecasts (ERA5) as the forcing dataset, which~~, which~~ benefits from decades of advancements in data assimilation, core dynamics, and model physics (Hersbach et al., 2020)~~, is used to drive both the WAM-2layers and FLEXPART-WaterSip~~~~two models~~. The moisture tracking simulations specifically target ~~time period for our simulations is~~ July 2022, a month significantly influenced by the ISM ~~in~~ in~~for~~ the TP region (Yao et al., 2013; Curio and Scherer, 2016). The ~~entire~~ moisture tracking domain spans from ~~30~~30°S~~–~~ to 80°N and from ~~40~~40°W to ~~–140~~140°E, covering nearly all potential oceanic and terrestrial source regions of ~~the TP~~ precipitation over TP (Chen et al., 2012; Li et al., 2022a). ~~In both simulations, t~~In the simulations,~~he~~ ~~YB and UTB~~the two representative basins ~~areas~~ are represented ~~by~~ with gridded boundaries as shown in Fig. S1 in the Supplement. Considering the number of particles released, data size, and computational resources needed, both models are driven by~~we use~~ 1°×1° and 3-hourly ERA5 data~~ to drive both models~~, although some specific variables used in the two models are different due to their distinct ~~underlying~~ physical mechanisms.

In WAM-2layers, ~~targeted~~ tagged moisture is continuously released into Eulerian grids and tracked as it ~~gradually~~ progressively accumulates and ~~persistently~~ diffuses ~~between~~ across grids over time. The ~~targeted~~ tagged moisture ~~is~~ was released throughout the entire July (from 31-July to 1-July in ~~the~~ backward mode), ~~and~~ with the backward tracking period ~~extends~~ extending back to 1 June. A previous study in the TP region ~~reported~~ demonstrated that a ~~period of~~ ~30 ~~30~~-day~~s~~ tracking period can ensure that ~~around~~ approximately 95% of the tagged moisture returns to the ground (Zhang et al., 2017), which is ~~also~~ consistent with our numerical experiments in the YB and UTB (Fig. ~~S~~2a). In comparison, FLEXPART-WaterSip model ~~traces~~ tracks atmospheric particles released at each step independently, thereby avoiding interference between particles released at different times. This differs from WAM-2layers, ~~where~~ which ensures that in FLEXPART-WaterSip moisture released at ~~different~~ various times does not converge~~s~~ into the same set of Eulerian grids. ~~Consequently~~Typically, ~~scientists typically set~~ the average residence time of moisture in the atmosphere (~10 days) is used as the ~~moisture~~ tracking period for a single particle release ~~of particles~~ in FLEXPART-WaterSip. To align the ~~ensure a consistent~~ tracking duration and maximize the tracking of ~~the tracking of the~~ ta~~rgeted~~gged moisture in both models (Fig. ~~S~~2), the backward tracking time in FLEXPART-WaterSip was ~~set~~ extended to 30 days. For FLEXPART-WaterSip, although large deviations in actual air parcel movements may occur beyond the average 10-day residence time ~~(~10 days)~~, the ~~increasing~~ associated uncertainties in trajectories beyond this period are ~~not expected~~unlikely to substantially ~~affect~~ impact the results, as the majority of moisture uptake occurs within the first 10 days (Sodemann et al., 2008). Our numerical experiments, as illustrated in Fig. ~~S~~2b, indicate that within the first 10 days (20 days), we traced 89% (99%) of the precipitation moisture in the YB and 97% (99%) in the UTB. ~~The d~~Detailed configurations of WAM-2layers and FLEXPART models can be found in Part 2 of the Supplement~~ary Part 2~~,. The WaterSip source code ~~and the reference codes for WaterSip (our self-written codes in Python)~~we developed in this study can be found in Part 3 of the Supplement~~Supplementary Part 3~~.

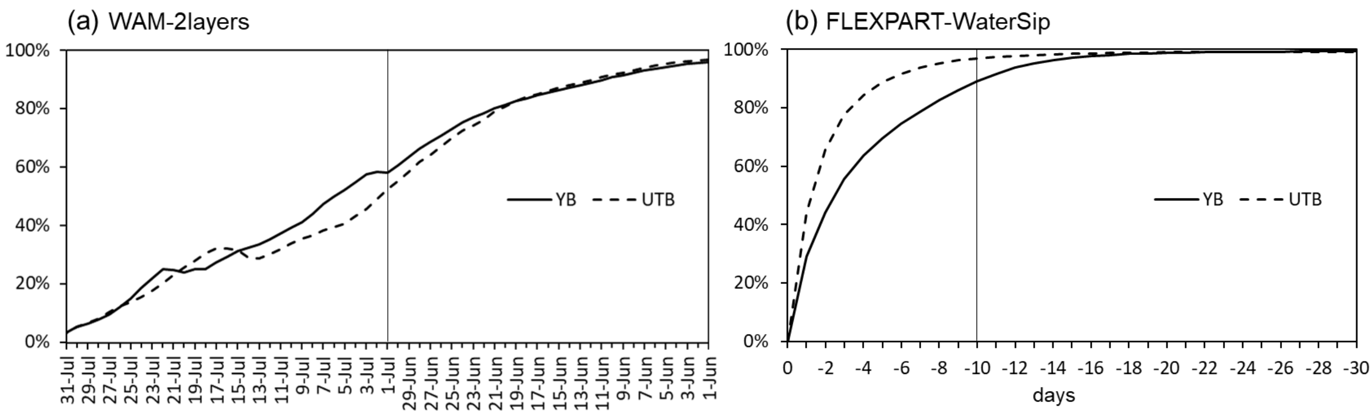

Figure 2. Backward moisture tracking periods and accumulated moisture uptake from all source regions~~.~~ in (a) ~~for~~ WAM-2layers and (b) ~~for~~ FLEXPART-WaterSip models. Solid lines represent the ~~YB~~YB, and dotted lines represent the UTB.

3 Moisture tracking in two ~~typical~~ representative basins ~~using the Eulerian and Lagrangian methods~~

Figure ~~2~~ 3 shows the simulated moisture sources ~~of~~ for precipitation in July 2022 over the YB and UTB based on WAM-2layers and FLEXPART-WaterSip models. Moisture contributions are ~~represented~~ quantified as equivalent water height (mm) over the source ~~areas~~regions. For the YB, ~~I~~in addition to significant local recycling, the distribution of most moisture sources ~~for YB precipitation primarily follow~~aligns with the path of the ISM ~~path~~, ~~traversing~~ extending from the southern slope~~s~~ of the Himalayas, through the Bay of Bengal (BB),) and the Indian subcontinent, and to the Arabian Sea (AS), extending and reaching as far asto the Southern Indian Ocean (SIO) (Figs. 2a 3a and c). Meanwhile, the Mmoisture sources for the UTB precipitation mainly stretch along the westerlies to the Central Asia region (Figs. 2b 3b and d). Generally, in comparison with FLEXPART-WaterSip, WAM-2layers simulations exhibitssuggest a broader coveragerange of distant moisture sources from (including both the westerlies-dominated and ISM-dominated regions) when compared to those identified by FLEXPART-WaterSip.Spatially, notable disparities between the two models are most evident in the northwestern source region. Whether in the ISM-dominated YB or the westerlies-dominated UTB, FLEXPART-WaterSip, compared to WAM-2layers, exhibits only minimal moisture source contribution from the entire northwestern Eurasian continent and northeastern Atlantic. Another noteworthy detail is the clear north-eastward extension of moisture sources for UTB precipitation resolved by FLEXPART-WaterSip, reaching almost to the easternmost Tianshan Mountains (Fig. 2d), a feature absent in the results of WAM-2layers (Fig. 2b).

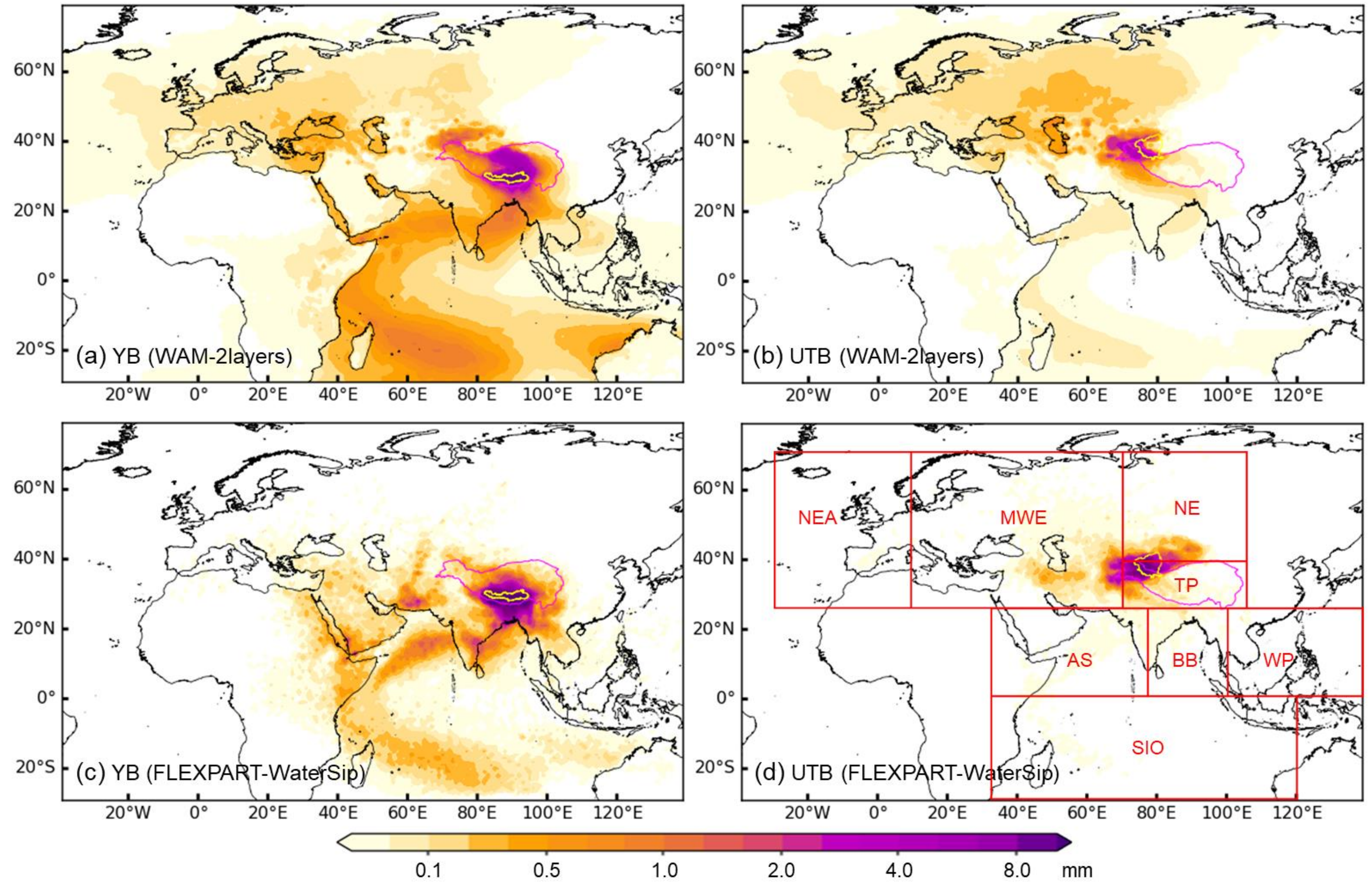

(a) YB (WAM-2layers)
(b) UTB (WAM-2layers)
(c) YB (FLEXPART-WaterSip)
(d) UTB (FLEXPART-WaterSip)
60°N
40°N
20°N
0°
20°S
20°W
0°
20°E
40°E
60°E
80°E
100°E
120°E
NEA
MWE
NE
TP
AS
BB
WP
SIO
0.1
0.5
1.0
2.0
4.0
8.0
mm

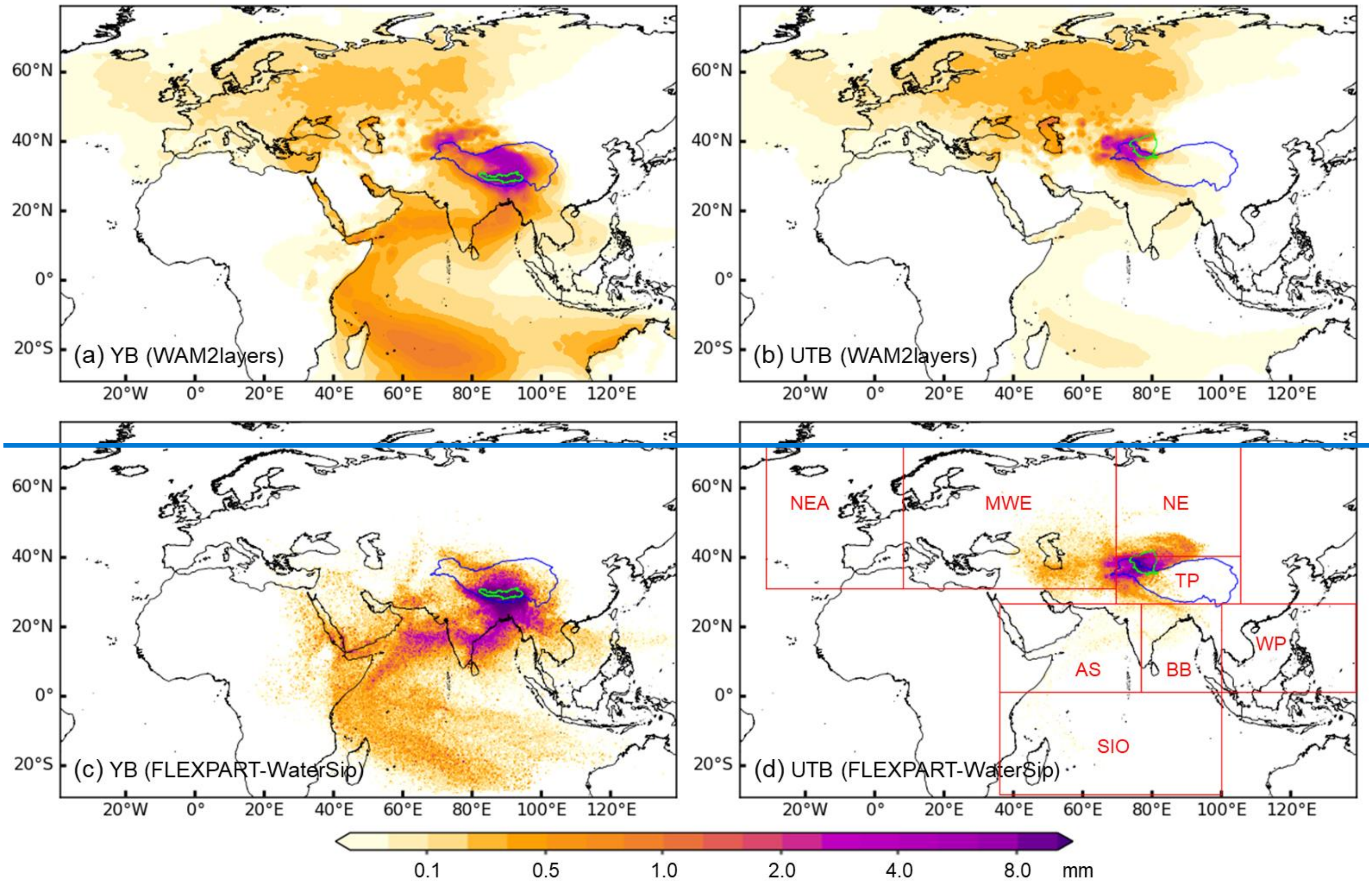

Figure 23: Spatial distributions of moisture contributions (equivalent water height over source areasregions; mm) to precipitation in July 2022 in the (a and c) the YB (a and c) and (b and d) UTB (b and d), simulated by (a and b) WAM-2layers (a and b) and (c and d) FLEXPART-WaterSip models (c and d). Blue Purple lines represent the TP boundary and cyan yellow lines represent the boundaries of the two representative basins. Red boxes in (d) delineate the division of the eight source regions: North-eastern Atlantic (NEA), Midwestern Eurasia (MWE), Northern Eurasia (NE), TP, Arabian Sea (AS), Bay of Bengal (BB), Western Pacific (WP), and Southern Indian Ocean (SIO).

The differences between the moisture tracking results from the two models are shown in Figure 3 illustratesWe calculate the differences in simulations based on the two models in Figure 4 (WAM-2layers minus FLEXPART-WaterSip). When eCompared to FLEXPART-WaterSip, WAM-2layers model tends to estimate a higher moisture contribution from the westerlies-dominated northwestern source regions for both basins, spanning . This extends from nearby sources (regions to the northwest of the YB and to the west of the UTB) to distant sources across the entire northwestern Eurasian continent and northeastern Atlantic. Additionally, WAM-2layers model estimates higher greater moisture contributions from large parts of the Indian Ocean, particularly the distant Southern Indian OceanSIO in the YB simulation. In contrast, lower contributions estimated by WAM-2layers are mainly occur infrom local and nearby source regions downwind of the westerlieslocated opposite to the westerlies direction, i.especifically. around the southern slopes of the Himalayas in the YB simulation and the entire Tarim Basin in the UTB simulation. Another noteworthy detail isNotably, Notably, aroundover the Red Sea and Persian Gulf regions, WAM-2layers simulations model estimate indicates higher moisture contributions from the oceans but lower moisture contribution from the surrounding land areas, s than FLEXPART-WaterSip, in exhibit an underestimation of moisture contribution in certain scattered areas compared to FLEXPART-WaterSip, especially in the YB simulation (Fig. 3a4a). These disparities discrepancies between the two moisture tracking models remain are consistent in both in absolute and relative terms (Figs. 3 4 and S3S2).

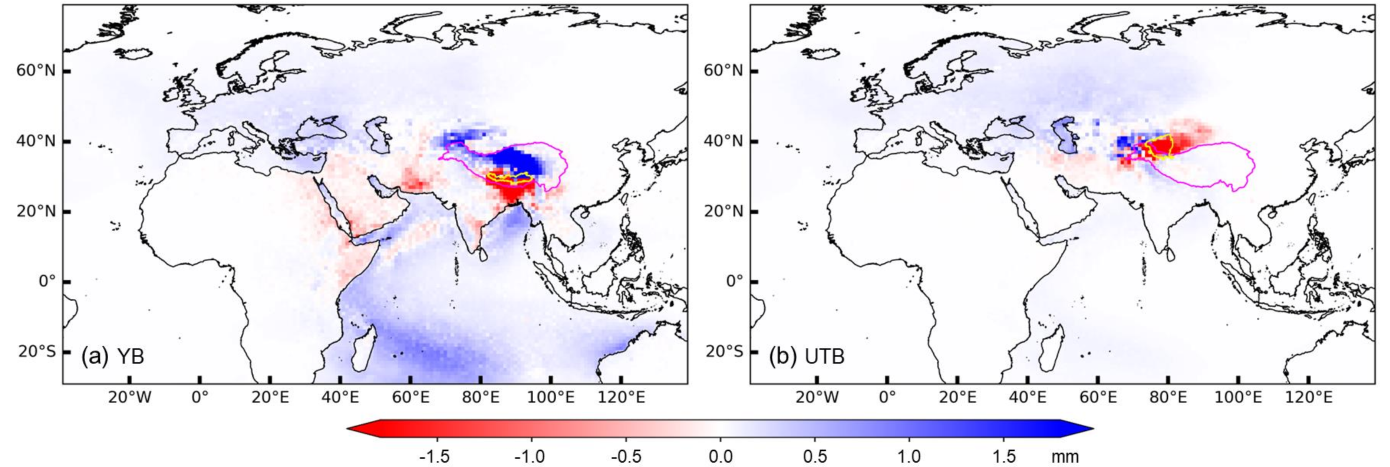

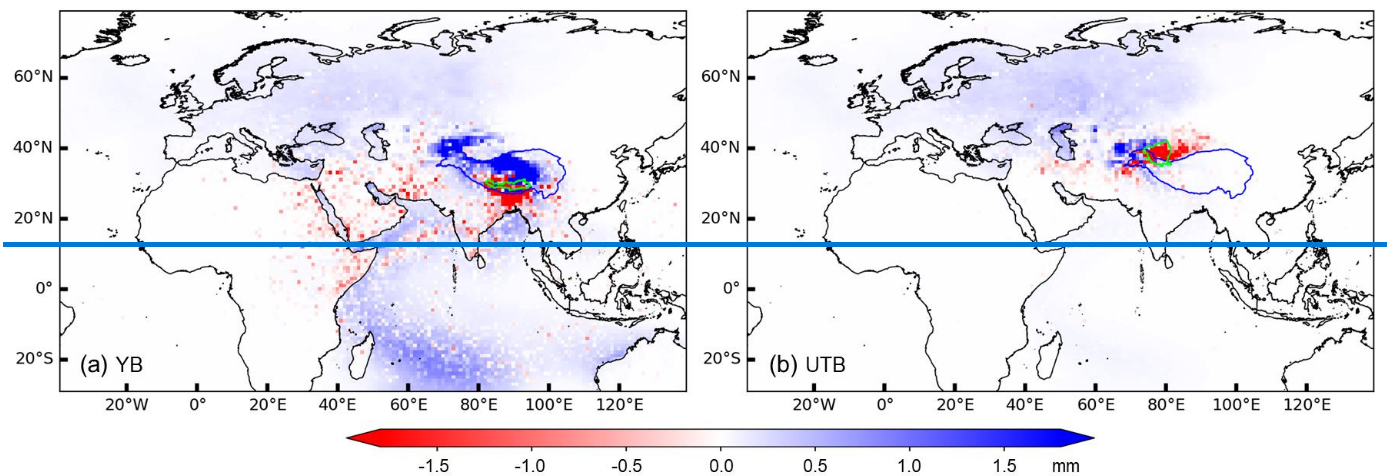

Figure 34: Absolute differences in moisture contributions between between WAM-2layers and FLEXPART-WaterSip the two simulations simulations (WAM-2layers minus FLEXPART-WaterSip) forfor in the the (a) YB (a) and (b) UTB simulations (b).

Considering the distribution of moisture sources, eight critical source regions (~~as indicated by~~see the red boxes in Fig. ~~2d~~3d) are selected for further quantitative analysis. Figure ~~4~~ 5 shows the relative contributions from the~~se~~ eight ~~moisture source~~~~selected~~critical regions and ~~the rest~~remaining regions to precipitation in the YB and UTB~~ precipitation~~. Both models indicate that the major moisture sources for the YB are local recycling and the ISM regions (TP, AS, BB, and SIO), whereas for the UTB, the primary sources are local recycling and ~~westerly~~ westerlies-influenced regions (TP, NE, and MWE). Specifically, WAM-2layers model estimates that the TP contributes ~~For moisture contribution~~ 32% of the moisture toward ~~from the TP to~~ the YB, ~~WAM-2layers estimates it at 35~~32~~%,~~ which is about two-thirds of the estimate by FLEXPART-WaterSip model (~~52~~53%). An even greater discrepancy ~~Even more substantial difference~~ is observed for the ~~estimated~~ contribution of the TP~~'s contribution~~ to the UTB, for which WAM-2layers model estimates 28% compared to FLEXPART-WaterSip's ~~: the relative contributions from TP are estimated to be 24~~28~~% by WAM-2layers but 68~~72%~~ by FLEXPART-WaterSip~~. For distant sources, the SIO is the most representative one for the YB, with WAM-2layers estimating its contribution at ~~26~~30%, compared to only ~~(cf.~~ 11~~0~~% ~~for~~ by FLEXPART-WaterSip~~)~~. ~~Meanwhile~~For the UTB, ~~, for~~ the MWE~~, the most~~ is a key ~~representative~~ distant source~~ of the UTB~~, with WAM-2layers ~~estimates~~ estimating a 36% contribution~~, (44~~36~~%)~~ ~~even triple~~doubling~~e~~ that calculated by FLEXPART-WaterSip (~~13~~15%). ~~In addition to the disparities showcased in Figs. 2 and 3, Fig. 4 quantitatively reveals that the differences between these two sets of simulations are considerably larger for the UTB than for the YB.~~In summary, ~~as~~ compared to FLEXPART-WaterSip, WAM-2layers model ~~tends to~~generally estimates higher moisture contributions from the westerlies-dominated sources ~~and~~as well as distant sources, but lower contributions from local recycling and nearby sources downwind of the westerlies~~opposite to the westerlies direction~~.

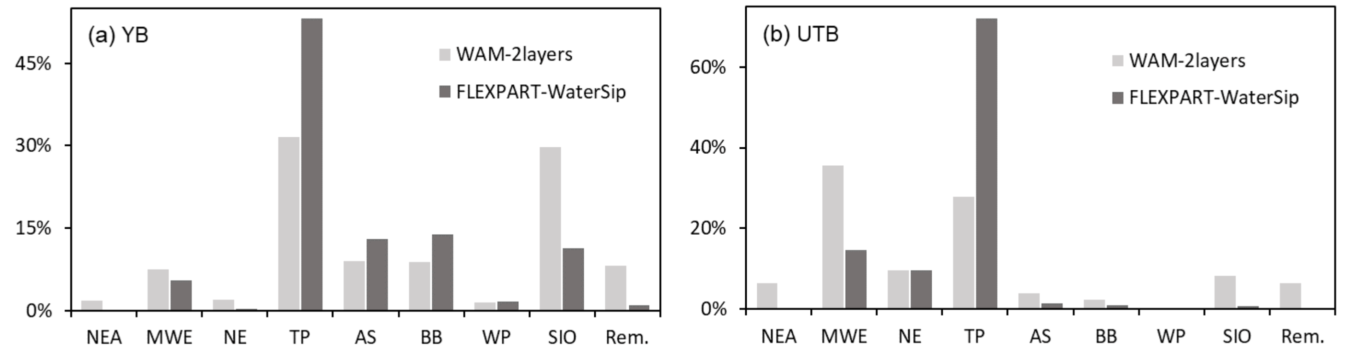

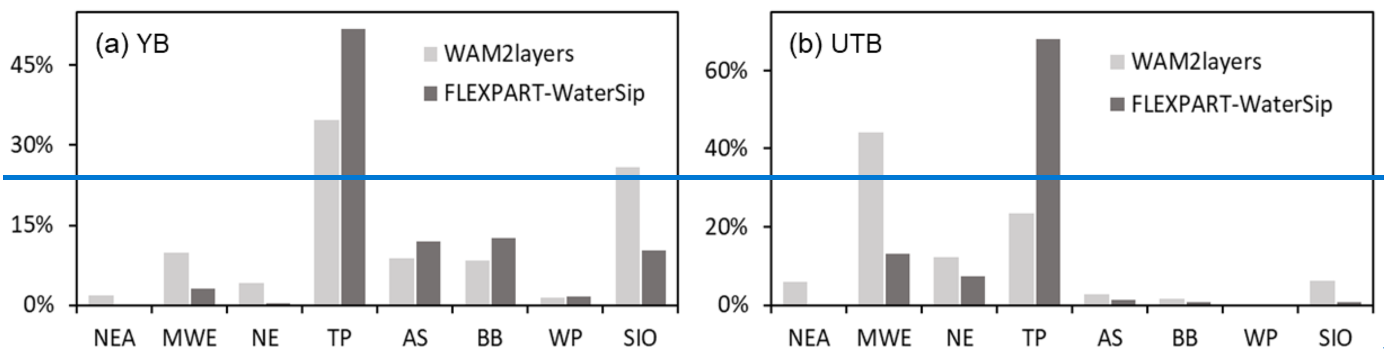

Figure 45: Relative moisture contributions (%) to precipitation over the the(a) YB (a) and (b) UTB (b) from the eight selected source regions (NEA, MWE, NE, TP, AS, BB, WP, and SIO) and the restremaining (Rem.) source regions, simulated by WAM-2layers and FLEXPART-WaterSip models.

To further evaluate potential disparities between the two models, we specifically identified a day with maximum precipitation in July, representing an instance of extreme precipitation events, for additional moisture tracking simulations. Based on the daily precipitation time series of the two basins (Fig. S4), the extreme precipitation events in YB and UTB occurred on 21-July and 14-July, respectively. Figure S5 shows the simulated moisture sources of these two events using WAM-2layers and FLEXPART-WaterSip, while Figs. S6 and S7 show the spatial and regional differences between the two simulations (WAM-2layers minus FLEXPART-WaterSip). In addition to differences in absolute contribution amounts, the spatial distributions of moisture sources and the spatial differences between the two models for these extreme events in the YB and UTB are generally consistent with those for the entire July (Figs. S5–6; cf. Figs. 2–3). Meanwhile, the relative contributions from the eight selected sources in Fig. S7 closely match those in Fig. 4. In general, simulation disparities between the two models are less pronounced in the ISM-dominated YB than in the westerlies-dominated UTB. The most notable characteristic of WAM-2layers, as compared to FLEXPART-WaterSip, is that it tends to estimate higher moisture contribution from the westerlies-dominated sources and distant sources but lower contribution from local recycling and nearby sources opposite to the westerlies direction.

4 Moisture fluxes in ~~Eulerian method~~WAM-2layers and particle trajectories in ~~Lagrangian method~~FLXPART-WaterSip simulations

When tracing moisture sources, WAM-2layers model primarily utilizes horizontal moisture fluxes in the upper and lower atmospheric layers ~~(divided at ~810 hPa at a standard surface pressure; see Fig. 1a)~~ to determine the ~~backward transport of~~ water vapor transport from ~~the target region to~~ global sources to the target region in a backward mode. Figure 6 illustrates t~~T~~he average moisture transport fluxes in the two layers during the entire simulation period as estimated by WAM-2layers ~~are shown in Fig. 5~~6. The ISM-dominated moisture transport to the TP region primarily occurs in the lower layer, whereas the westerlies-dominated moisture transport to the region is mainly from the north in the lower layer and from the west in the upper layer, a phenomenon pronounced in the northwest vicinity of the UTB.

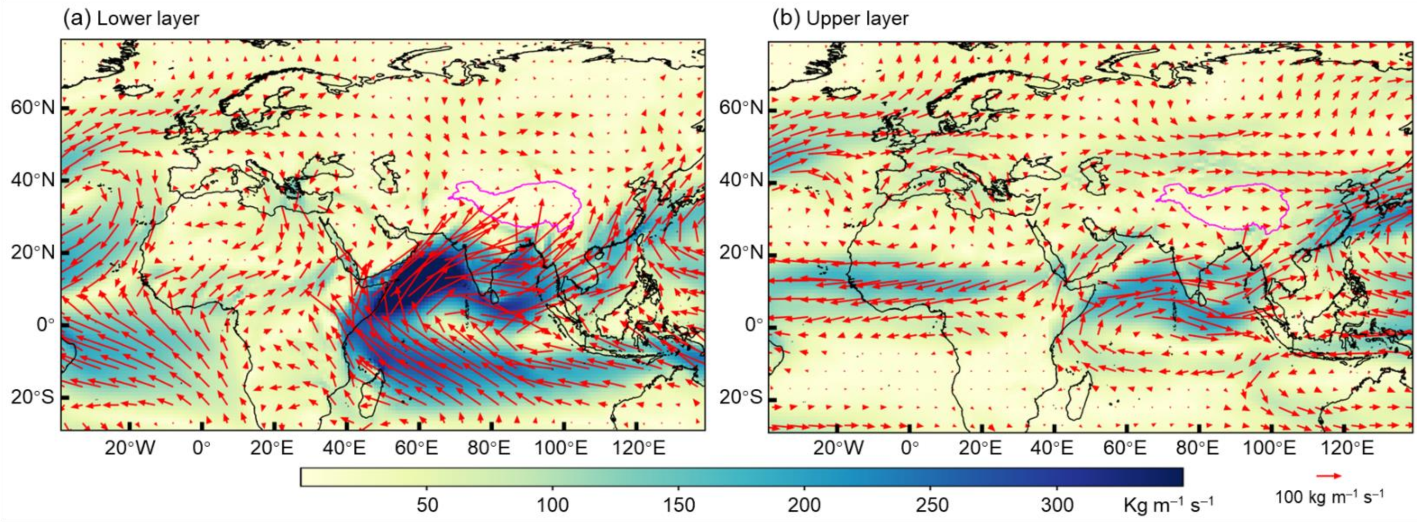

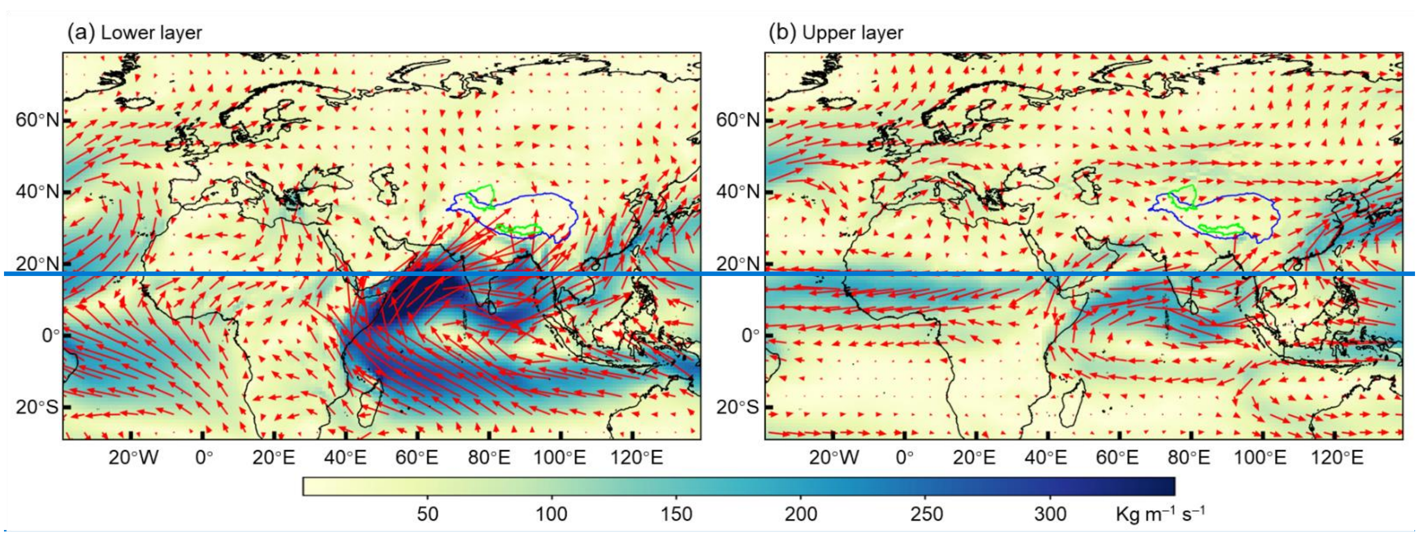

Figure ~~5~~6: Average moisture transport fluxes (kg m^{-1} s^{-1}) in the (a) lower ~~(a)~~ and (b) upper ~~(b)~~ layers in ~~the~~ WAM-2layers during the entire simulation period.

In comparison, FLEXPART outputs ~~extensive~~ detailed information on air particles and trajectories critical to ~~, providing valuable insights into~~ diagnosing moisture sources. Figure ~~6~~ 7 shows the spatial distributions of particles and trajectories ~~that bring moisture~~contributing to precipitation over the YB and UTB in the FLEXPART-WaterSip simulation. It should be noted that the particles and trajectories in Fig. ~~6~~ 7 are clustered results using the K-means clustering method for clearer graphical representation, reducing ~~(~~ the number of particles ~~reduced~~ by a factor of 100~~,~~ and the number of trajectories by a factor of 150~~)~~,. This treatment ~~which~~ may have filtered out some chaotic and distant particles and trajectories. In Lagrangian backward simulations, ~~Particles~~ particles released from the YB predominantly travel south~~-~~westward, ~~whereas~~ while those from the UTB primarily spread westward (Fig~~s~~. 7a and b). Within about 15 days, the traced particles can ~~transport from target regions to~~reach the farthest ~~end of the~~ source regions. ~~As suggested by t~~The results of backward tracking days suggest~~, there are~~ approximately three distinct~~,~~ fastest moisture transport paths to the YB:~~.~~ ~~(red arrows in Fig. 6a~~i.e. the northwestern route from the MWE, the southwestern route from the AS, and the southeastern route from the WP~~),~~ . ~~while t~~The most pronounced moisture transport path to the UTB is confined to western routes ~~(red arrow in Fig. 6b)~~. ~~Another notable observation~~Additionally, there is a notable ~~is the~~ rapid north~~-~~eastward transport of tracked particles in the UTB over a short period after release (Fig. ~~6~~7b~~,~~ and Fig. 3d ~~also illustrates the expansion of moisture sources to this direction~~), a phenomenon indiscernible ~~challenging to discern~~ in ~~the~~ WAM-2layers simulations (Fig~~s~~. ~~2~~3b and d and Fig. 6) ~~and its two-layer moisture transport fluxes (Fig. 5)~~. This phenomenon may be associated with the complex and variable convective activities as well as the simulation biases in the region, as indicated by ~~Upon a brief examination of~~ the vertical wind patterns at ~~850 hPa and 500 hPa~~different pressure levels across the study domain (Fig. S3 in the Supplement) ~~and take into account the complex motion is difficult to identify under the overall averaged Eulerian grids, we guess that this phenomenon may be associated with the complex and variable convective activities in the region~~ and~~.~~ ~~However, in this study, our exploration has been limited to the founding that this phenomenon is to some extent attributable to~~ the overestimat~~ioned~~ ~~of~~ local evaporation ~~by~~in FLEXPART-WaterSip (see Sections 5 and 6).

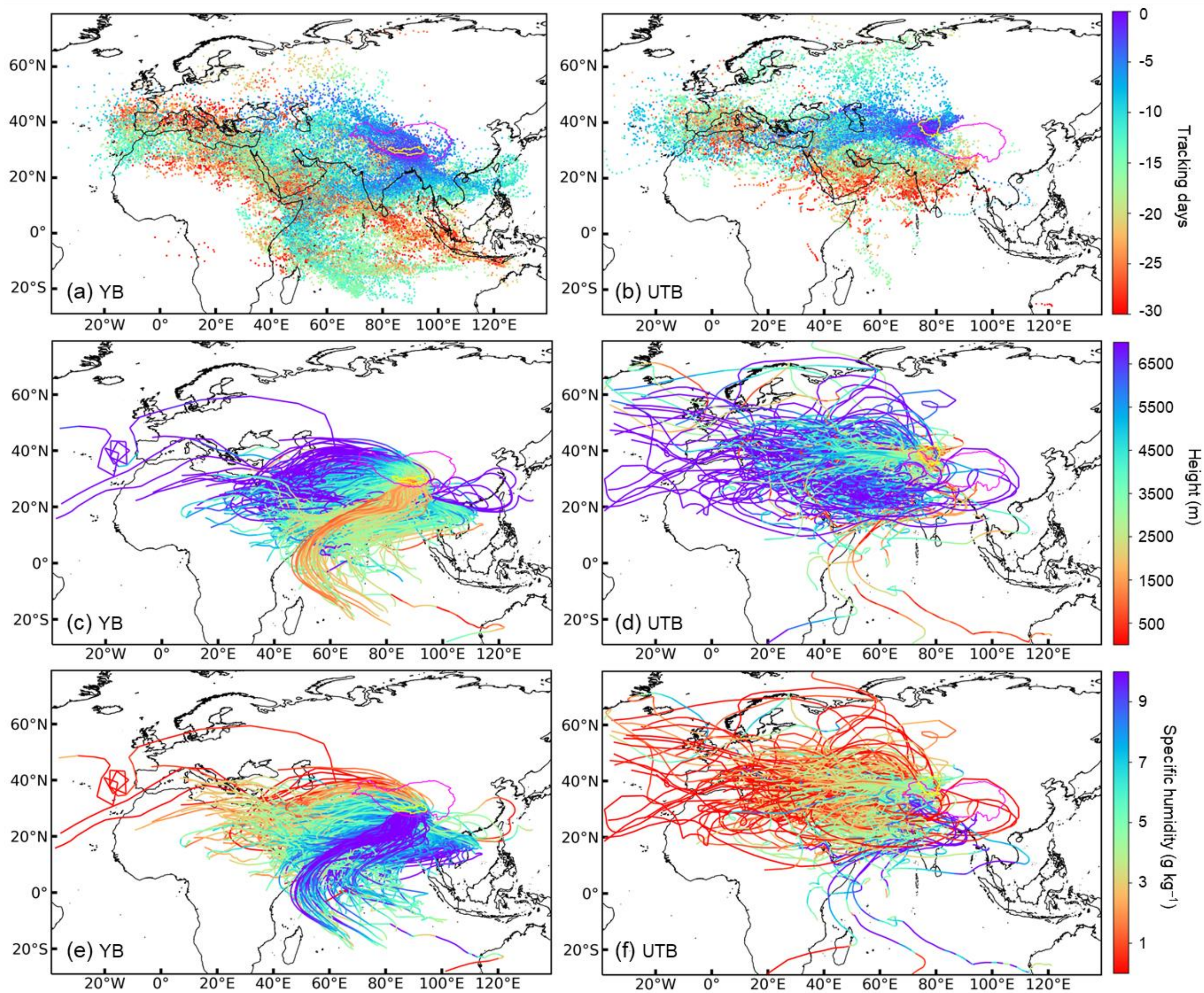
(a) YB
(b) UTB
(c) YB
(d) UTB
(e) YB
(f) UTB
60°N
40°N
20°N
0°
20°S
20°W
0°
20°E
40°E
60°E
80°E
100°E
120°E
Tracking days
0
-5
-10
-15
-20
-25
-30
Height (m)
6500
5500
4500
3500
2500
1500
500
Specific humidity (g kg⁻¹)
9
7
5
3
1

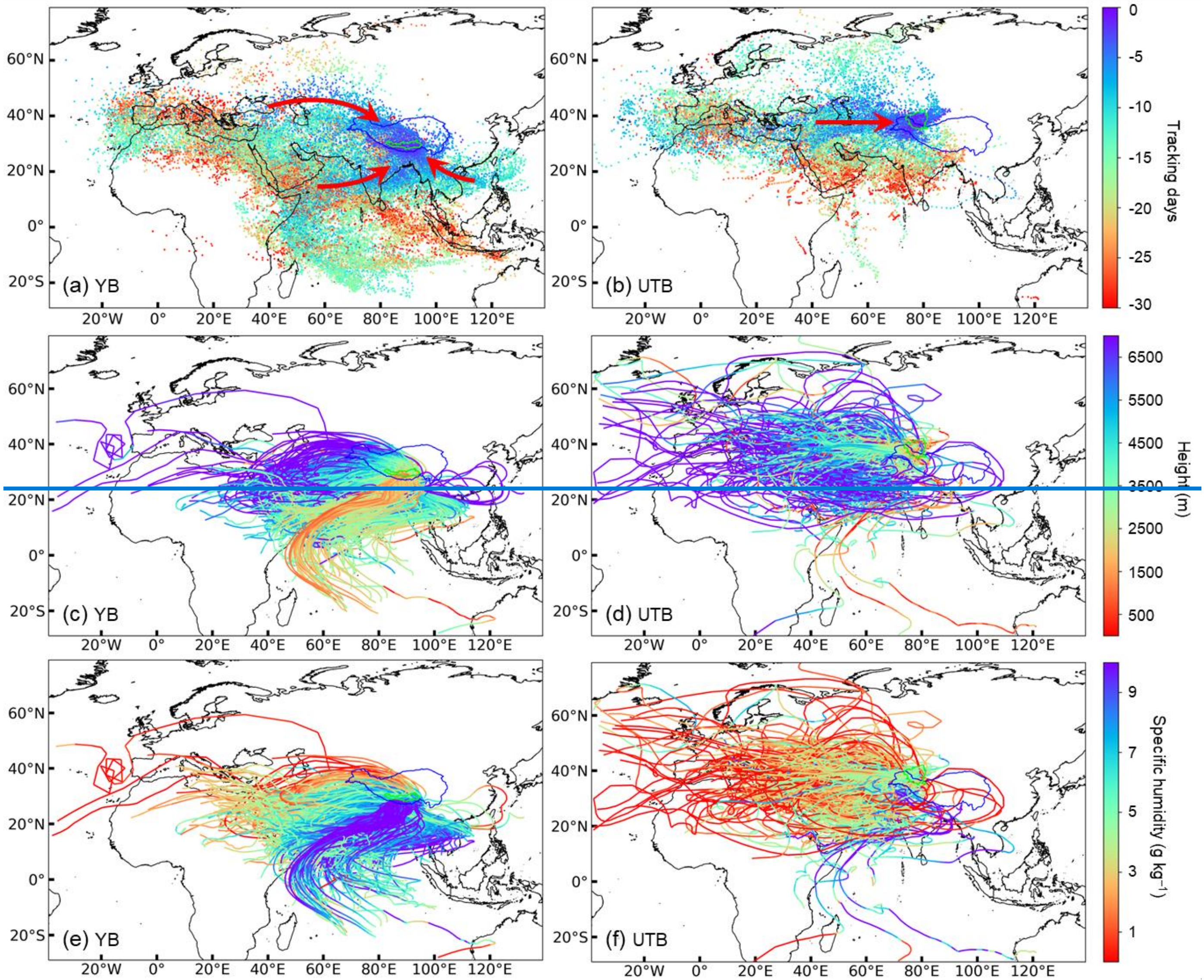

Figure ~~6~~7: Spatial distributions of (a and b) particles ~~(a and b)~~ and (c–h) trajectories ~~(c–h)~~ that ~~bring~~ transport moisture to ~~precipitation over~~ the (a, c, and e) YB ~~(a, c, and e)~~ and (b, d, and f) UTB ~~(b, d, and f),~~ as simulated ~~by~~ in FLEXPART model~~.~~: (a and b) ~~are~~ particles color-coded by backward-tracking days (0–30 days~~).~~), (c and d) ~~are~~ trajectories color-coded by height (m, above ground) at each numerical step~~.~~, and (e and f) ~~are~~ trajectories color-coded by specific humidity (g kg^{-1}) at each numerical step.

~~Another notable observation is the rapid north-eastward transport of tracked particles in the UTB over a short period (Fig. 6b), a phenomenon challenging to discern in the WAM-2layers simulations (Figs. 2b and d) and its two-layer moisture transport fluxes (Fig. 5). This suggests the capability of FLEXPART model to capture smaller scale atmospheric processes that may not~~

be as apparent in the Eulerian model. Upon closer examination of the vertical wind patterns at 700 hPa and 300 hPa across the study domain (Fig. 7), we observed more complex and variable convective activities near the UTB compared to those around the YB. This further implies that the modelling capability of WAM-2layers for moisture sources of the UTB may be less robust than for the YB, consistent with the observation that the simulation disparities between the two models are more pronounced in the UTB than that in the YB (Fig. 4). The vertical wind patterns in Fig. 7 also explain another phenomenon around the Red Sea and Persian Gulf regions. The spatial distributions of moisture sources simulated by WAM-2layers show a consistent alignment with the land–sea boundaries (see Figs. 2a–b and Figs. S5a–b). This corresponds with the common understanding that greater evaporation (over oceans) means a higher potential for moisture contribution to the target region. However, in FLEXPART-WaterSip simulations, terrestrial sources with high moisture contributions are widely distributed around the Red Sea and Persian Gulf (Figs. 2c–d), accompanied by enhanced upward motion compared to the adjacent oceanic regions (Fig. 7). Essentially, FLEXPART-WaterSip detects only the increases in specific humidity, possibly in the mid-to-upper atmosphere caused by strong land convection, while the actual sources of these increased moisture might still be the strong evaporation from oceans. In this regard, the estimation from WAM2-layers is more reasonable than that from FLEXPART-WaterSip.

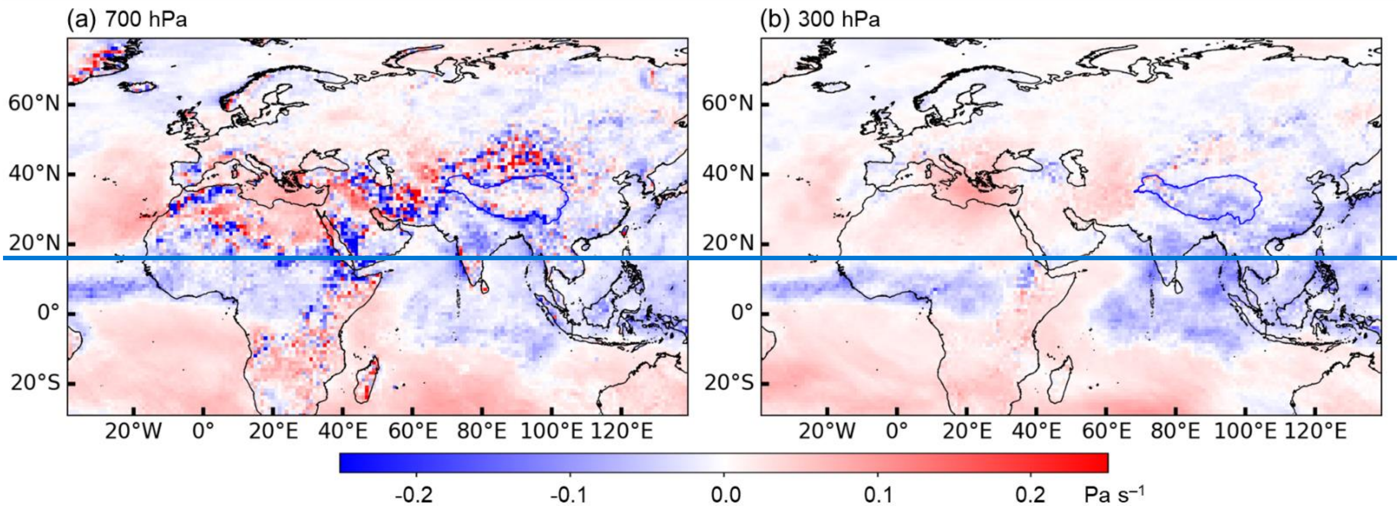

Figure 7: Atmospheric vertical velocities (Pa s^{-1}) at 700 hPa and 300 hPa across the entire study domain. Note the negative values indicate upward motion (ascent).

In terms of trajectories iAs suggested in Figs. 6c7c–d, those trajectories originating from the western sources are mainly typically at higher altitudes, (some even exceeding 6000 m), but they undergo a notabley descent descend in altitude before reaching the target region, forming a strip-like lower atmospheric transport channel in the western part of the target region. This is in general consistent with WAM-2layers simulations, in whichConsidering the upper-layer horizontal moisture transport in WAM-2layers, the upper layerof moisture originating from the northwestern Eurasian is also higher than that in the lower layer (Fig. 56). For In comparison, trajectories from the ISM-dominated sources, they are at relatively lower altitudes, with some originating from the SIO even descending below 1000 m. Generally, the moisture-carrying capacity of these trajectories correlates with both their altitude and the moisture conditions in their source regions. In conjunction withAs shown in Figs. 6e–f, trajectories originating from the ISM-dominated regions and lower altitudes exhibit higher moisture content, whereas those from the westerlies-dominated regions and higher altitudes are characterized by lower moisture content.

A notable difference between WAM-2layers and FLEXPART-WaterSip simulations, as highlighted illustrated in Fig. 24, is that the spatial extent ofexpansion of moisture source regions identified in -FLEXPART-WaterSip is not as extensive asmuch smaller than in WAM-2layers, especially over thein distant sourcesregions, such as model fails to capture most moisture source regions across the entire northwestern Eurasia-. for both basins when compared to WAM-2layers. SpecificallyIn Fig. 6, pParticle trajectories simulated by FLEXPART (see Fig. 6) are only sparsely distributed across northwestern Eurasia, particularly for the YB (Fig. 7). This inconsistency is also evident when comparing results from previous studiesprevious studies using WAM-2layers (Zhang et al., 2017; Li et al., 2022a) and FLEXPART-WaterSip (Chen et al., 2019; Yao et al., 2020). This indicates that the underestimated moisture contributions from these westerlies-dominated northwestern Eurasiadistant sources in FLEXPART-WaterSip, as compared to WAM-2layers, is are largely attributed due to a reduced lower proportion of air particles originating from this these source regions reaching the target region.

5 Relationship between “actual actual evaporation” and simulated moisture source contributions

A common understanding onIn general, for moisture source––receptor diagnosisistics is that inwithin a specific source region, areas with higher evaporation rates generally contribute more moisture to the target region than areas with lower evaporation rates, especially in source regions where the differencecontrast between oceanic and terrestrial evaporation is pronounced. To further investigate the relationship between evaporation and simulated moisture contributions from various source regions, we employ evaporation data from ERA5 as the benchmark (“actual evaporation”; Fig. 8a) for the entire tracking period (June–July 2022). IAs shown in Figs. 33 and 8a, we have observed that the distributions of moisture sources simulated by WAM-2layers aligns more closely with the general pattern of global evaporation patterns from ERA5 (oceanic evaporation rates surpassexceed those of surrounding terrestrial areas) compared to that by FLEXPART-WaterSip. This alignment is particularly evident in the sources aroundin the Red Sea and Persian Gulf regions, where theone of the most pronounced differencediscrepancies between the two models is observed in moisture sources between ocean and land is pronounced between the two models (Fig. 44a). FLEXPART-WaterSip model generally captures the spatial pattern of evaporation across oceanic regions but largely overestimates terrestrial evaporation from mid- and low-latitudes (e.g., the Middle East, Mediterranean, and Indian subcontinent regions; all of which are critical source regions for the two basins). These findings are consistent with a previous long-term, global scale study by Keune et al. (2022). Although FLEXPART-WaterSip demonstrates potential in capturing complex local atmospheric processes, the bias in simulated evaporation can inevitably affect the quantification of moisture source–receptor dynamics.

The vertical wind patterns in Fig. 7 also explain another phenomenon around the Red Sea and Persian Gulf regions. The spatial distributions of moisture sources simulated by WAM-2layers show a consistent alignment with the land–sea boundaries (see Figs. 2a–b and Figs. S5a–b). This corresponds with the common understanding that greater evaporation (over oceans) means a higher potential for moisture contribution to the target region. However, in FLEXPART-WaterSip simulations, terrestrial sources with high moisture contributions are widely distributed around the Red Sea and Persian Gulf (Figs. 2c–d), accompanied by enhanced upward motion compared to the adjacent oceanic regions (Fig. 7). Essentially, FLEXPART-WaterSip detects only the increases in specific humidity, possibly in the mid-to-upper atmosphere caused by strong land convection, while the actual sources of these increased moisture might still be the strong evaporation from oceans. In this regard, the estimation from WAM2-layers is more reasonable than that from FLEXPART-WaterSip.

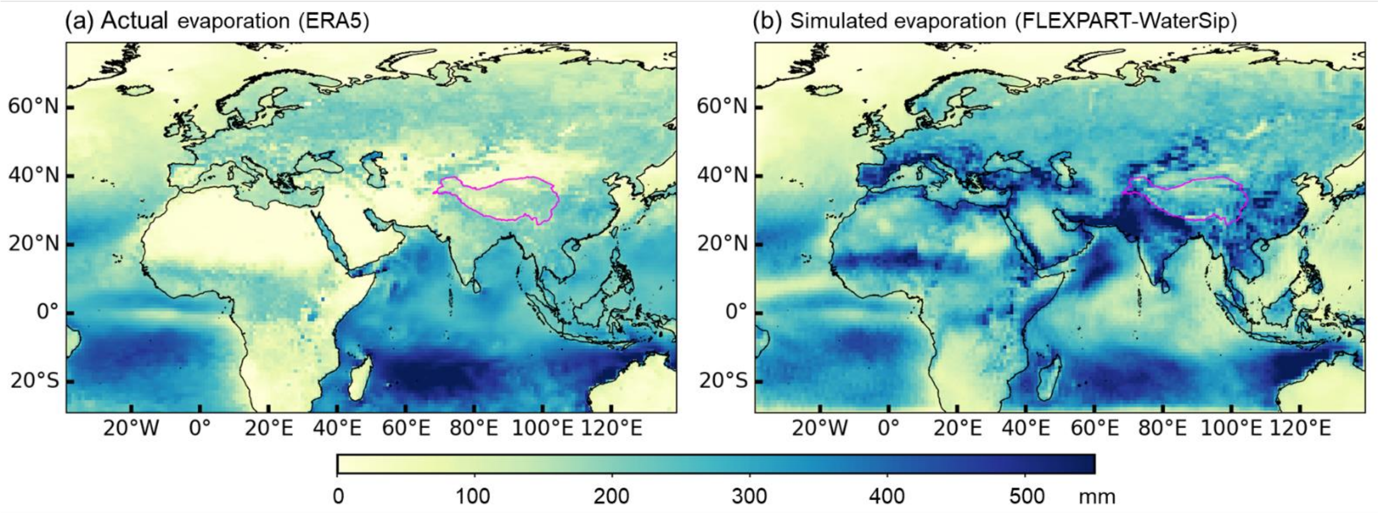

Figure 8: (a) "Actual evaporationEvaporation " from ERA5 and (b) simulated evaporation from FLEXPART-WaterSip during June–July 2022.

We furtherthen detectexamine the relationships between "actual evaporation" and simulated moisture contributions inacross all grid cells in the eight selected source regions, as scatter plots displayed in (Fig. S4). It i's clearobvious that, for both the YB and UTBbasins, the positive correlations between "actual evaporation" and moisture contributions appears mainly appears in the WAM-2layers simulations, particularlyespecially in the westerlies-dominated NEA and MWE as well as the ISM-dominated AS and SIO regions, where(the relevant correlation coefficients all exceed 0.3). In contrast, in the FLEXPART-WaterSip simulations rarely show, strong positive correlations between "actual evaporation" and moisture contributions from source areas are rarely observed. One of the mostA striking examples is around the Red Sea and Persian Gulf regions, where oceanic evaporation is notably higher than terrestrial evaporation (Fig. 8a). As mentioned above, However, FLEXPART-WaterSip model appearsseems to have missinadequately captured the relatively high evaporation moisture over the Red Sea, Persian Gulf, and eastern Mediterranean (see Fig. 33c), despite there is a large number ofextensive tracking particles coveringin these areasregions (see Fig. 77a). We speculate that the complex atmospheric activitiesstrong moisture contrast between land and ocean the complex local circulation systems in these regions, as (partially illustratedevidenced by vertical velocities in Fig. S3 in the Supplement,) may leadcontribute to these issues in moisture source diagnosis using thein WaterSip method. To further illustrate the underlying mechanisms, we randomly selected two representative trajectories: one from the SIO to the YB, and the other from the NEA to the UTB (Fig. S45 in the Supplement). Comparisons between model outputs and ERA5 data, as shown in Fig. S56 in the Supplement, suggest that the modeled changes in specific humidity for particles may not fully reflect the actual processes of precipitation and evaporation both in the lower and upper atmosphereduring the moisture transport. Relying solely on specific humidity changes and particle height to assess evaporation, precipitation, and moisture transport can be quite challenging. Although the WaterSip method employs thresholds (e.g., 1.5 BLH and 0.2 g^{-1} kg^{-1} every 6 h for specific humidity changes) to exclude a large number of potential misdiagnoses over the source regions, further advancements in diagnostic and correction methods are still needed.For example, intense tropical convection continuously lifts lower atmospheric moisture to upper levels and forms precipitation, while strong surface evaporation consistently replenishes moisture to the lower atmosphere. During this process, even though substantial evaporation enters the lower atmosphere, it may not be fully reflected by changes in specific humidity. Additionally, changes in specific humidity in the lower atmosphere may not effectively capture the moisture loss associated with precipitation in the upper-level. In this context, we conducted a simple test wherein we randomly selected two typical trajectories: one originating from the SIO leading to precipitation in the YB, and another originating from the NEA responsible for precipitation in the UTB (Fig. S4). Leveraging the high spatial-temporal resolution ERA5 data, we conducted a comprehensive analysis to these two trajectories (detailed analysis see Fig. S5). We argue that using specific humidity changes and particle height to assess evaporation, precipitation, and moisture transport over source regions remains challenging. Despite the WaterSip method have employed different thresholds (such ad 1.5 BLH and 0.2 g^{-1} kg^{-1} 6h^{-1} for specific humidity changes) to filter out a considerable number of potential erroneous diagnoses over the source regions, advancing methods for diagnosing and correcting associated errors remains imperative(Keune et al., 2022).

; mm; mmare results frommodel, while the third and fourth rows are results from models values

Similar to the moisture source-receptor diagnosis for precipitation particles in the target area, computing all released particles in the atmosphere would provide simulated evaporation over the entire tracking domain. Therefore, Fig. 8b displays the FLEXPART-WaterSip simulated evaporation over the tracking domain during the entire tracking period. In comparison with “actual evaporation”, FLEXPART-WaterSip model generally captures the spatial pattern of evaporation across oceanic regions but largely overestimates terrestrial evaporation from mid- and low-latitudes (e.g., surrounding the Mediterranean, the Middle East, and the Indian subcontinent; all of which are critical source regions for the two basins in the TP). FLEXPART-WaterSip model generally captures the spatial pattern of evaporation across oceanic regions but largely overestimates terrestrial evaporation from mid- and low-latitudes (e.g., the Middle East, Mediterranean, and Indian subcontinent regions; all of which

~~are critical source regions for the two basins).~~ These findings are consistent with a previous long-term, global scale study by Keune et al. (2022). Although FLEXPART-WaterSip demonstrates potential in capturing complex local atmospheric ~~processes~~activities, the bias in simulated evaporation can inevitably affect the quantification of moisture source–receptor dynamics.

~~Similar to the moisture source-receptor diagnosis for precipitation particles in the target area, computing all released particles in the atmosphere would provide simulated evaporation over the entire moisture tracking domain. Therefore, Fig. 8b displays the FLEXPART-WaterSip simulated evaporation over the tracking domain during the entire tracking period. In comparison with "actual evaporation" (Fig. 8a), the model generally captures the spatial pattern of evaporation intensity across ocean areas. However, in the land areas of mid-low latitudes in the Northern Hemisphere, the simulated evaporation is notably overestimated. Particularly in the land areas surrounding the Red Sea, Persian Gulf, and Mediterranean, as well as between the Arabian Sea and the southern slopes of TP, these regions all serve as crucial moisture sources for the two basins. Actually, these comparison also align with the diagnosis results of evaporation simulation at a long-time and global-scale reported by Keune et al. (2022). Although FLEXPART-WaterSip exhibits the potential to capture complex local atmospheric processes, its simulation bias in evaporation inevitably affects the quantification diagnosis of moisture source-receptor processes. This observation is particularly important when these areas of significantly overestimated evaporation occur largely within the major moisture sources discussed in this study. Keune et al. (2022)~~

6 Bias correction of FLEXPART-WaterSip simulations

Keune et al. (2022) ~~have~~ introduced ~~a unified framework~~ the~~(~~ Heat And MoiSture Tracking framEwoRk (HAMSTER), a unified framework ~~aimed at~~designed to correct~~ing~~ ~~the~~ biases ~~of~~in moisture source~~-~~–receptor diagnos~~is~~tics ~~that relies on~~based on particle trajectories from Lagrangian model~~ simulation~~s~~,~~. This framework leverages ~~based on~~ the relationships between actual and simulated surface fluxes (~~include~~ evaporation and precipitation). ~~On the first step~~The first step, in line with WaterSip, is to~~, they utilize~~ use specific thresholds ~~of~~for specific humidity changes, relative humidity, and particle height to quantify ~~the~~ moisture source~~–~~–receptor ~~processes~~relationships ~~of~~for precipitation in the target ~~area~~region (~~they also introduced~~ a "random attribution" method was~~can~~ also introduced~~be applied~~). ~~Then,~~Subsequently, a first round of corrections is conducted by comparing actual and simulated precipitation in the target ~~area~~region~~, they perform the first round of correction on the quantification process~~ (i.e., bias correction of receptor variables). A second round of corrections then focuses on ~~Next, by~~ comparing actual and simulated evaporation ~~over th~~across all~~e entire~~ source regions~~, they conduct a second round of correction~~ (i.e., bias correction of source variables). Th~~is~~ese process~~es~~ aim~~s~~ to achieve ~~Ultimately, a~~ reasonable, bias-corrected moisture source contributions~~ will be obtained~~. ~~However~~It is noteworthy that~~,~~ the HAMSTER method does not include ~~a~~ calibration for the filtering thresholds of precipitation particles in the target ~~area~~region, ~~which may~~potentially leading to certain deviations in the spatiotemporal distribution of tracked particle trajectories. If actual precipitation data in the target region were used to calibrate the filtering thresholds of precipitation particles, the step of “bias correction of receptor variables”~~for preciptiation~~ in HAMSTER could be ~~omitted~~replaced. ~~If we use actual precipitation data in the target area to calibrate the filtering thresholds of precipitation particles, the second step in HAMSTER can be disregarded. Accordingly, its necessary to add a step to optimize the filtering thresholds of precipitation particles before conducting the moisture source diagnosis.~~ Inspired by the HAMSTER method, we ~~introduce~~develop a simplified two-step approach to~~for~~ correct~~ing~~ moisture tracking results from FLEXPART-WaterSip:

Step 1: Optimize the filtering thresholds of precipitation particles in the target ~~area~~region. ~~Based on~~Using the default precipitation particle filtering thresholds ~~of~~for specific humidity change (0.2 g kg^{-1}~~g/kg~~) and relative humidity (80%), we conducted numerical ~~separate tests~~experiments to examine how adjustments to these thresholds impact simulated precipitation ~~varies with changes in these thresholds~~. ~~I~~As shown in Fig~~s~~. 9a and b, ~~when fixing~~maintaining a constant ~~the thresholds of~~ relative humidity threshold at 80%~~,~~ while varying the ~~adjustments made to thresholds of~~ specific humidity change~~s~~ threshold from 0.05 to 0.2 g kg^{-1} results in a ~~led to~~ minimal ~~change~~decreases in simulated precipitation (~~with specific humidity thresholds increasing from 0.05 to 0.2 g/kg, the decrease in simulated precipitation is~~ less than 1 mm~~, across~~ for both basins). In contrast ~~(Figs. 10c and d)~~, ~~when~~ fixing the ~~thresholds of~~ specific humidity change threshold at 0.2 g kg^{-1}~~g/kg,~~ while ~~the adjustments made to thresholds of~~changing the relative humidity threshold leads~~led~~ to ~~significant~~substantial changes in simulated precipitation (Fig. ~~10~~9c and d). ~~Through the test~~Our experiments indicate that~~, we consider the~~ precipitation simulation is more sensitive to changes in the relative humidity threshold, with the optimal values of 63% for the YB ~~is 63%,~~ and 74% for the UTB ~~is 74%~~. This step ensures a more accurate selection of precipitation particles for subsequent moisture source diagnosis.

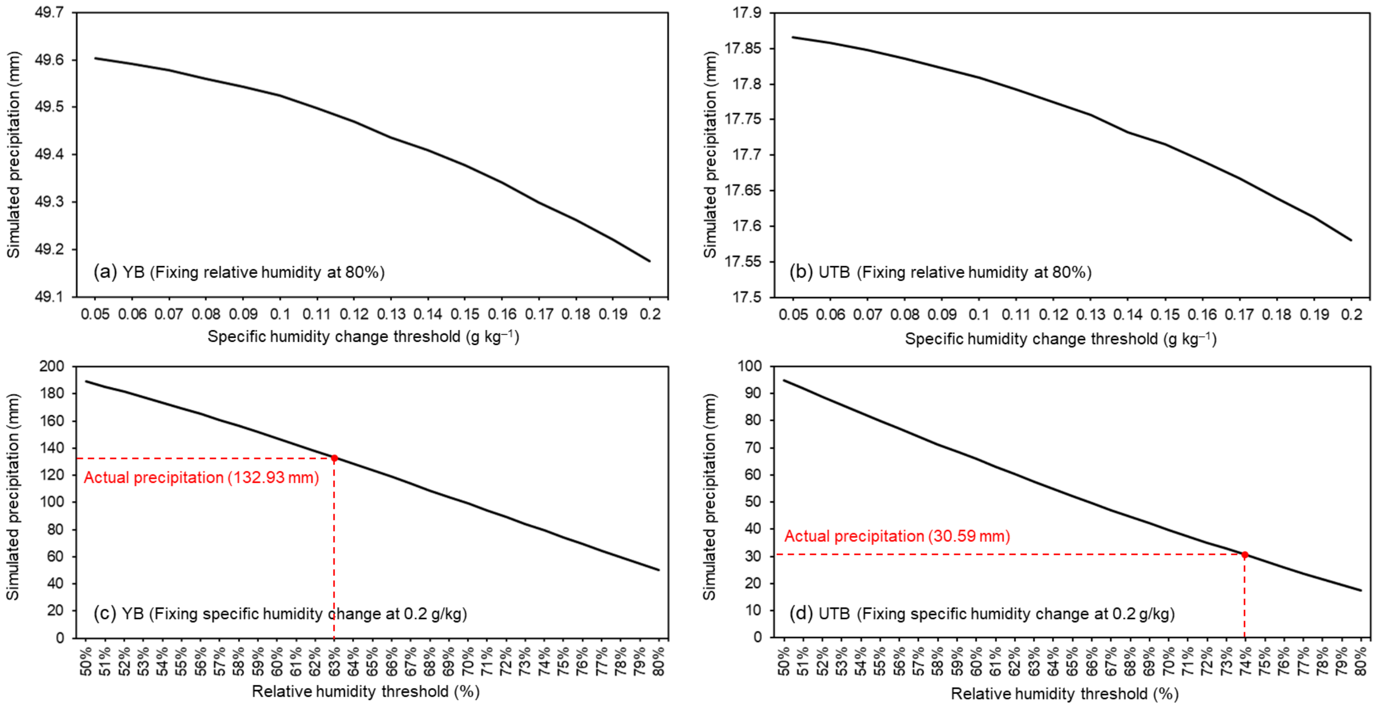

Figure 9: Sensitivity of the simulated precipitation in the (a and c) YB and (b and d) UTB to (a and b) the ~~experiments of~~ thresholds ~~in~~of specific humidity change ~~changes (a and b)~~ and (c and d) the threshold of relative humidity ~~(c and d) on simulated precipitation in the YB (a and c) and UTB (b and d) regions~~.

Step 2: Correct ~~the~~ biases ~~of~~in simulated evaporation over the source regions. First~~ly~~, ~~utilize~~use the optimized thresholds from ~~the first s~~Step 1 to quantify ~~the~~ moisture source contributions. ~~Then~~Next, calculate grid-scale correction factors by dividing actual evaporation ~~with~~by simulated evaporation ~~in~~for each grid cell~~s~~ over the entire moisture tracking period~~, we obtain the grid-scale correction factors~~ (Fig. S7 in the Supplement)~~,~~. These correction factors ~~which could~~are then applied ~~be used~~ to correct ~~the~~ moisture source contributions. This step ~~will correct~~addresses the simulation biases in evaporation ~~over~~across the moisture tracking domain ~~under~~when using the WaterSip ~~scheme~~method. It is important to ~~We should~~ note that although these correction factors are ~~bound~~likely to vary over time, ~~however,~~ this ~~aspect~~variability was not ~~taken into consideration~~accounted for in this ~~work~~ study due to the relatively short ~~time period~~simulation period. For~~When conducting~~ long-term moisture source diagnosis corrections, ~~utilizing~~implementing time-varying correction factors would be more appropriate.

~~In Figs. 11a and b, we calculate t~~The bias-corrected FLEXPART-WaterSip simulations for the YB and UTB, based on the two-step bias correction approach~~s above~~, are shown in Fig. ~~11~~10a and b. The bias correction ~~makes~~align the ~~simulation results of~~ FLEXPART-WaterSip simulation results more closely ~~more consistent~~ with the global pattern of ~~land-sea~~terrestrial and oceanic evaporation ~~differences~~, especially around the Red Sea and Persian Gulf regions. ~~Simultaneously~~Additionally, it enhances the moisture contributions from the high-latitude Eurasian continent and the Indian Ocean, while reducing ~~moisture~~ contributions from the western land areas in the mid- and low-~~-~~latitude (Fig. S7 in the Supplement). ~~Considering the bias-corrected simulations are relative reliability, w~~We further compare~~d~~ these bias-corrected simulations ~~them~~ with the original WAM-2layers and FLEXPART-WaterSip simulations, as shown in Fig~~s~~. 10c–~~d and Figs. 11e–~~f~~, respectively~~. The differences depicted in Fig~~s~~. 10c–d are generally consistent with those ~~shown~~ in Fig. 4, indicating that WAM-2layers model tends to estimate higher moisture contributions from the westerlies-dominated sources and distant sources, but lower contributions from local recycling and nearby sources downwind of the westerlies~~opposite to the westerlies direction,~~ for both the YB and UTB. Compared to the bias-corrected results, ~~For~~ the original (uncorrected) FLEXPART-WaterSip simulations~~,~~ ~~in~~for the YB ~~(Fig. 11e), they~~ estimate lower moisture contributions from ~~the~~areas surrounding ~~of~~ the target region and ~~the entire southern~~ oceanic source regions, but ~~estimate~~ higher contributions from the western land areas (Fig. ~~11~~10e). ~~Conversely, i~~F~~n~~or the UTB ~~(Fig. 11f)~~, the uncorrected FLEXPART-WaterSip simulations mainly estimate higher moisture contributions from the target ~~are~~regiona and its surrounding ~~region~~areas (Fig. ~~11~~10f), ~~which also includes~~including the north-eastward ~~expansion~~stretch of moisture sources observed in Fig. 3d. Th~~is~~ese comparisons ~~indicate~~demonstrates that through bias correction, the original discrepancies in reflecting actual evaporation ~~simulation errors~~ between ~~FLEXPART-WaterSip and~~ WAM-2layers and FLEXPART-WaterSip simulations ~~have been~~can be significantly ~~corrected for the northeast moisture sources of the UTB~~mitigated.

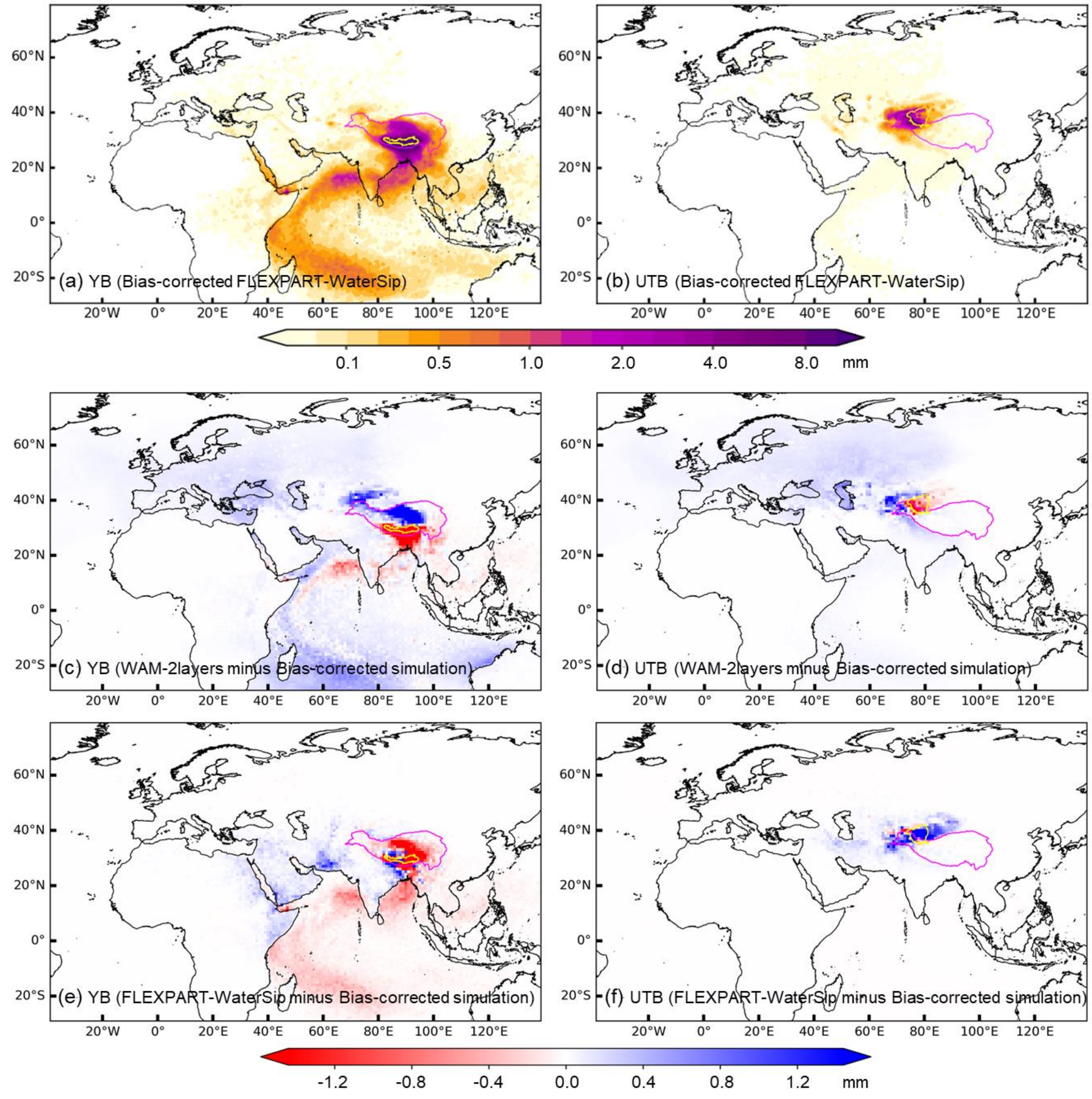

Figure 10: (a and b) Spatial distributions of bias-corrected moisture contributions (equivalent water height over source regions; mm) to precipitation in July 2022 in the (a) YB (a) and (b) UTB (b),simulated by based on FLEXPART-WaterSip simulationsmodel. (c–

f) Absolute differences in moisture contributions between original WAM-2layers/FLEXPART-WaterSip simulations and bias-corrected FLEXPART-WaterSip simulations for the (c and e) YB ~~(c and e)~~ and (d and f) UTB ~~(d and f)~~.

~~5~~ 7 Potential determinants of ~~disparities~~ discrepancies in moisture tracking ~~based on the Eulerian and Lagrangian methods~~

We now turn to a more comprehensive~~ and in-depth~~ examination of the ~~disparities~~ discrepancies observed in ~~Sections 3 and 4~~the original WAM-2layers and FLEXPART-WaterSip simulations. Considering the underlying physics of the models, forcing datasets, parameter selections, and our computational ~~capabilities~~resources, we designe~~d~~ ~~three~~ four ~~types~~sets of numerical experiments to ~~examine~~ investigate potential factors ~~influencing~~ contributing to the discrepancies ~~disparities~~ in~~-~~ different simulations~~ based on WAM-2layers and FLEXPART-WaterSip~~.

Experiment 1 – model resolution: ~~The s~~Simulation of moisture sources ~~by~~ using WAM-2layers is essentially a dynamic reproduction of moisture transport conditions ~~from~~ based upon forcing datasets, which means that the ~~simulation~~ accuracy heavily depends on the spatial~~-~~ and temporal resolutions of input data. ~~In this numerical experiment~~~~Apart~~In addition to~~ from~~ the original settings (1°×1° at 3-hourly resolution), we ~~set~~introduce three additional configurations of ERA5 data to determine whether improved spatial and/or temporal resolutions in forcing data could provide more accurate moisture source attributions: ~~(~~1°×1° at hourly resolution, 0.25°×0.25° at 3-hourly resolution~~s~~, and 0.25°×0.25° at hourly resolution~~s) of~~ ~~replace the 1°×1° and 3-hourly forcing data with 0.25°×0.25° and hourly ERA5 data to examine whether improved forcing dataset~~ spatial or temporal ~~resolutions~~ in forcing dataset ~~contribute to more detailed moisture source attributions~~. ~~Particularly, we examine whether this change would impact the higher moisture contribution from distant source regions estimated by WAM-2layers.~~ The ~~newly generated simulation~~ results from these additional simulations~~Results of this experiment~~ are summarized in Fig. ~~S8~~S8 in the Supplement.~~.~~

Experiment 2 – moisture source diagnosis thresholds: Quantifying ~~the~~ moisture source~~-~~–receptor ~~processes~~relationships in FLEXPART-WaterSip ~~depend~~hinges on the diagnos~~e~~is of potential precipitation particles and ~~source~~ evaporation sources, which in turn ~~rely~~depends on a ~~series~~set of threshold settings. Previous studies have suggested that ~~These settings have been considered to have different~~ optimal configurations for these thresholds may vary ~~in different parts around the world~~globally (Sodemann et al., 2008; Fremme and Sodemann, 2019; Keune et al., 2022). ~~Apart from~~In addition to the original setting (a relative humidity threshold ~~is~~of 80% and a specific humidity change threshold ~~is~~of 0.2 g kg^{-1}~~g/kg~~), we introduce~~set~~ one additional configuration for precipitation particles selection using th~~(th~~e optimized relative humidity threshold for the YB and UTB ~~are~~ ~~(~~63% and 74%, respectively), and two additional configurations for ~~source~~ evaporation source identification ~~(~~with specific humidity change threshold set at 0.1 and 0 g kg^{-1}~~g/kg)~~. The ~~newly generated simulation~~ results from these additional simulations are summarized in Fig. S9 in the Supplement.

Experiment 2 3 – number of particles: Using particle trajectories for Employing a source diagnostics methodology based on particle trajectories inevitably confines limits the identified moisture sources to these trajectories. ThereforeConsequently, a lower number of trajectories may result in potential inaccuracies, particularly when representing small to medium-scale atmospheric processes. This numerical experiment is designed to determine We are interested in understanding whether the relatively sparse particle trajectories over distant source regions would could introduce substantial uncertainties when estimating moisture contributions in FLEXPART-WaterSip. In this numerical experiment, we decrease reduce the number of particles initially released in FLEXPART from five million to one million. RThe resultss of this experiment are are summarized in Fig. S9 S10 in the Supplement.

Experiment 3 4 – "areal source–receptor attribution" methodmoisture source diagnosis: Different from the "WaterSip" method proposed by Sodemann et al. (2008), which attributes precipitation at a specific point within the target region to moisture uptake from multiple points along the trajectories, Sun and Wang (2014) introduced the "areal source–receptor attribution" method, focusing on a regional rather than a point scale. The "areal source–receptor attribution" method aims to calculates the total moisture contribution from an examinedn examined source to precipitation over across the entire target region instead of, as opposed to at specific points. This method allows forIt facilitates the differentiation of distinguishing moisture contributions from within and outside the examined sources along the trajectories. The basic framework diagram forof the "areal source-receptor attribution" method is shown in Fig. S11 in the Supplement, and the detailed methodology can be found(see in Sun and Wang (2014) for detailed methodology). In this numerical experiment, we utilize apply "areal source–receptor attribution" method to quantify moisture contributions from the eight source regions.

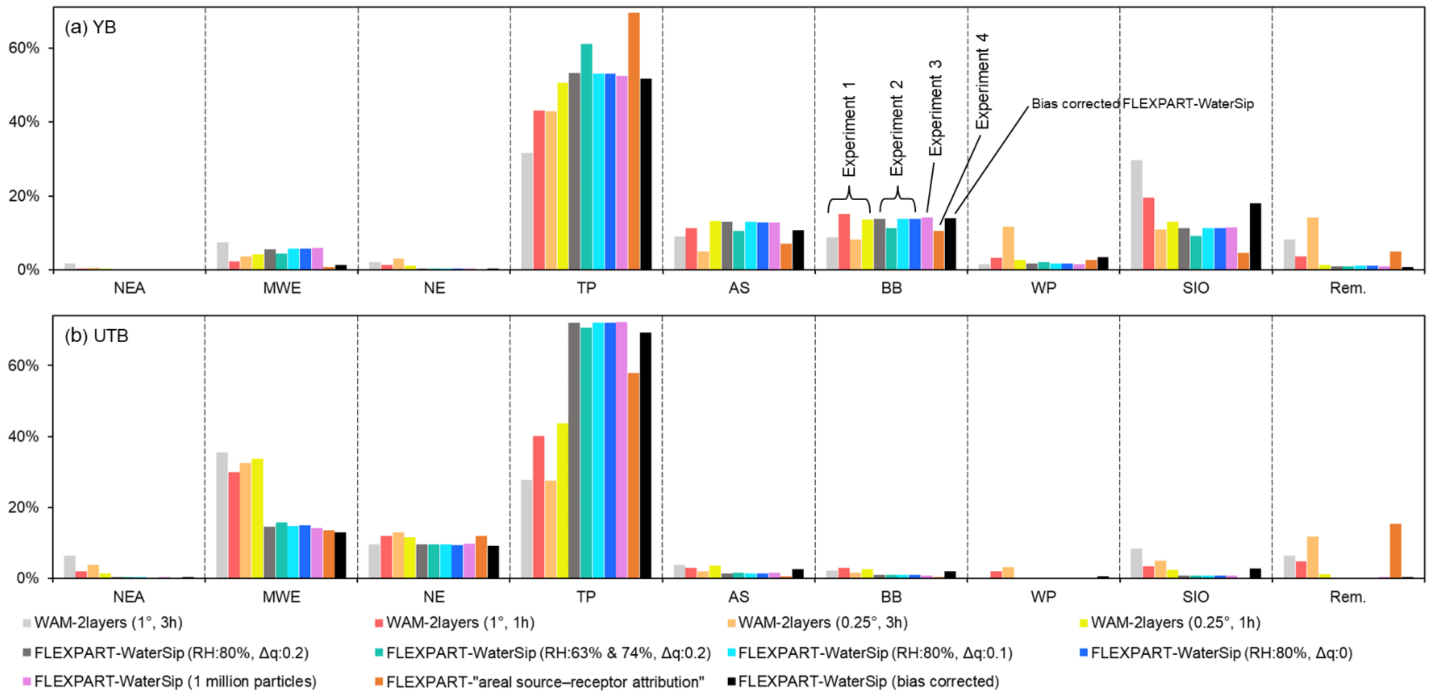
(a) YB
(b) UTB
0%
20%
40%
60%
NEA
MWE
NE
TP
AS
BB
WP
SIO
Rem.
Experiment 1
Experiment 2
Experiment 3
Experiment 4
Bias corrected FLEXPART-WaterSip
WAM-2layers (1°, 3h)
WAM-2layers (1°, 1h)
WAM-2layers (0.25°, 3h)
WAM-2layers (0.25°, 1h)
FLEXPART-WaterSip (RH:80%, Δq:0.2)
FLEXPART-WaterSip (RH:63% & 74%, Δq:0.2)
FLEXPART-WaterSip (RH:80%, Δq:0.1)
FLEXPART-WaterSip (RH:80%, Δq:0)
FLEXPART-WaterSip (1 million particles)
FLEXPART-"areal source–receptor attribution"
FLEXPART-WaterSip (bias corrected)

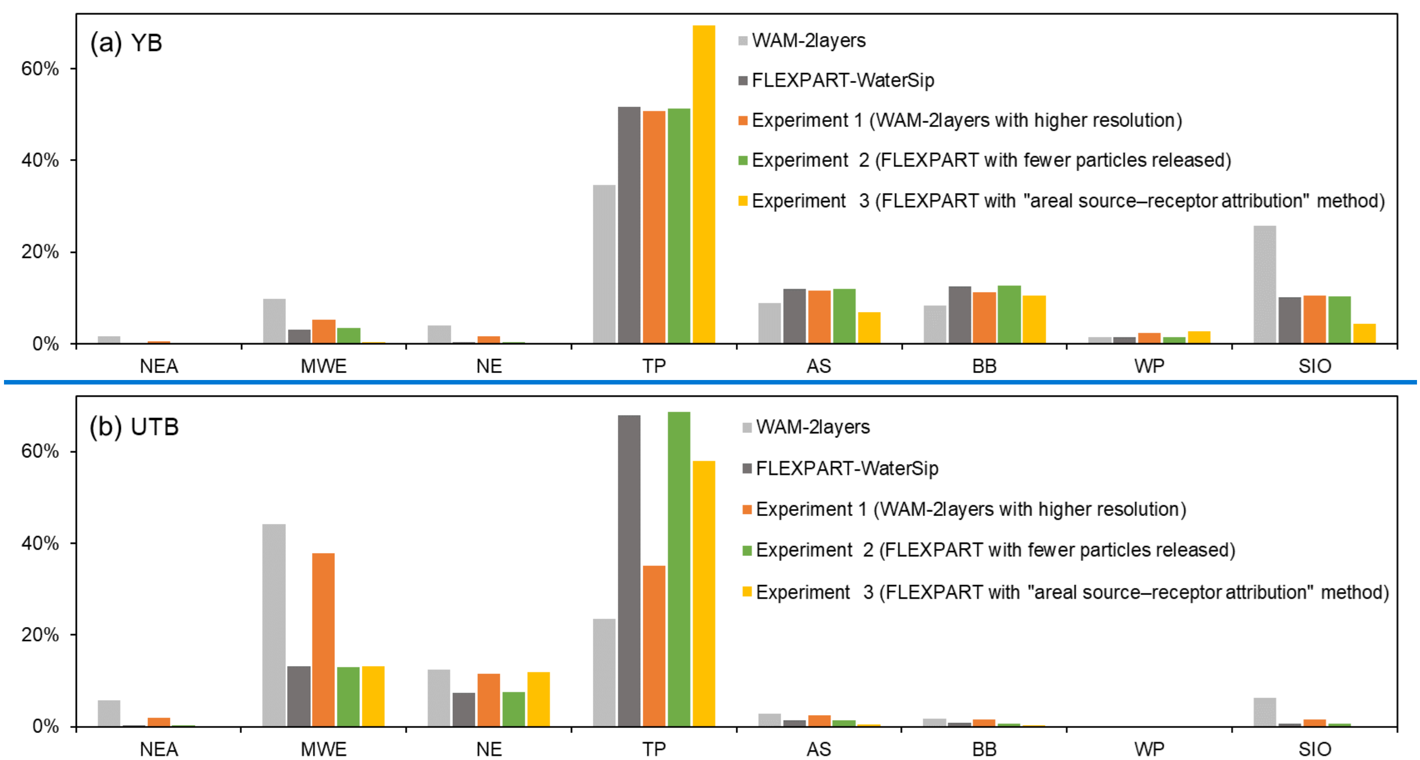
(a) YB
(b) UTB
0%
20%
40%
60%
NEA
MWE
NE
TP
AS
BB
WP
SIO
WAM-2layers
FLEXPART-WaterSip
Experiment 1 (WAM-2layers with higher resolution)
Experiment 2 (FLEXPART with fewer particles released)
Experiment 3 (FLEXPART with "areal source–receptor attribution" method)

Figure 118: Relative moisture contributions (%) to precipitation over the (a) -YB (a) and (b) UTB (b) from the eight selected source regions and the restremaining (Rem.) source regions, simulated by the four typesfour sets of numerical experiments (including the different configurations in WAM-2layers and FLEXPART-WaterSip, and FLEXPART- "“areal source–receptor attribution”") as well as, and the bias-corrected the original WAM-2layers and FLEXPART-WaterSip) simulations. The bBlack histograms represent the bias-corrected FLEXPART-WaterSip simulations. RH and Δq represent relative humidity threshold (mm) and specific humidity change threshold (g kg^{-1}), respectively. methods and the three numerical experiments.

Figure 8 11 shows the relative moisture contributions of from the eight selected source regions and the rest remaining source regions to the YB and UTB, in the in three the four typesset of numerical experiments and the bias-corrected FLEXPART-WaterSip simulations. The results for eachand the original simulations from both models (each source region comprisesincludes 11 sets of simulations, including the original simulations in Section 3 and the bias-corrected simulations in Section 6as in Sections 3 and 4). In Experiment 1, increasing the spatial- and temporal resolutions of the forcing dataset in general has broughtaligns the WAM-2layers (0.25° , 1h) simulations (Figs. S7e – f) more closerly with to the original bias-corrected FLEXPART-WaterSip (e.g., see results with 0.25°×0.25° at hourly resolution in Fig. S78e and f in the Supplement) simulations, particularly in infor the YB. For nearby sources, tThe moisture contributions from the TP to the YB (UTB) increases from 3532% (2428%) to 51% (3544%). For distant source regions, the moisture contributions from the MWE and SIO and MWE to the YB (UTB) decrease from 10% (44%) to 5% (38%) and from 2630% (68%) to 1113% (2%) and from 7% (36%) to 5% (34%), respectively. Our Ssensitivity experiments conduct separately for temporal and spatial resolutions reveal that increasing temporal resolution (from 3h to 1h) contributes more tosubstantially enhancinges the reliability of moisture source simulations (Figs. S8a–b in the Supplement). In contrast, solely increasing spatial resolution (from 1° to 0.25°) may lead to a stronger eastward extension of moisture sources for both basins (Figs. S8c–d in the Supplement), which is inconsistent withcontradicts to the WAM-2layers (0.25°, 1h) and bias-corrected FLEXPART-WaterSip results. In generalOverall, Experiment 1 revealsdemonstrates that enhancingimproving the spatiotemporal resolutions of forcing data in WAM-2layers can mitigate the issues of underestimation inof nearby sources and overestimation inof distant sources in the twofor both basins of the TP, particularly ifor then YB.

The moisture contribution from TP to the YB (UTB) increases from 35% (24%) to 51% (35%). For distant source regions, the moisture contributions from the MWE and SIO to the YB (UTB) decrease from 10% (44%) to 5% (38%) and from 26% (6%) to 11% (2%), respectively. A closer inspection of the spatial differences between Experiment 1 and original WAM-2layers simulations (Fig. 9) reveals that increasing model resolutions effectively reduces moisture contributions from distant source regions for both basins. However, this experiment fails to distinguish between simultaneous overestimation and underestimation in source regions around the two basins; instead, it results in enhanced moisture contributions from local and nearby sources.

In Experiment 2, correctingadjusting the thresholds of relative humidity significantlysubstantially enhances the overall moisture contributions from the source regions to the twoboth basins of the TP, butyet it has littleminimal effect on the spatial patterns of moisture sources (Figs. S9a–b in the Supplement). Sensitivity experiments regardingon specific humidity change thresholds of specific humidity change suggestshow only a slightminimal impact on moisture source simulations for the two basins (Figs. S9c–f in the Supplement). Generally, adjustingmodifying the thresholds of moisture source––receptor diagnosisistics does not seems not to improvereduce the potential biases in the spatial distributions of moisture sources, as when compared to the bias-corrected FLEXPART-WaterSip. In Experiment 3, Results from Experiment 2 closely resemble the original FLEXPART-WaterSip simulation (Figs. 8, S9, and S10), yet reducing the number of released particles to certain extentsomewhat limits our ability to discern finer details in the spatial distribution of moisture sources (Fig. S10 in the Supplement) (Fig. S9), butalthough the quantified Results from Experiment 2moisture contributions closely resemble those in the original the original FLEXPART-WaterSip simulations simulation (Figs. 8, S9, and S10), yetwith 500w5 million released particles. In In Experiment 4 demonstrates that , unlike, . In Experiment 3, the “areal source–receptor attribution” method, when compared to the original FLEXPART-WaterSip simulation, estimates reduced TP moisture contribution to the UTB but enhanced contribution for the YB. Iin contrast to the “WaterSip” method, the “areal source–receptor attribution” method utilizes all simulated trajectories for moisture source diagnosesdiagnosis, which may accumulate errors in trajectories that do not lead toresult in precipitation in the target region. Reapplying the “areal source–receptor attribution” method with trajectories filtered by the “WaterSip” method can produce moisture contributions that align more closely align with the original FLEXPART-WaterSip estimation estimates (results not shown).

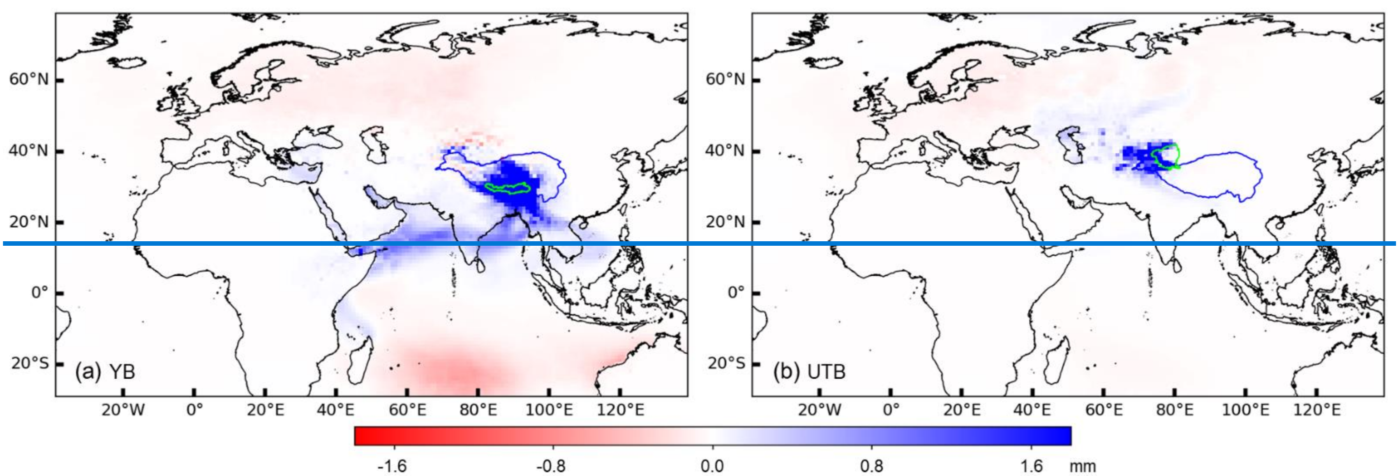

Figure 9: Absolute differences in moisture contributions between Experiment 1 and original WAM-2layers simulations (Experiment 1 minus original WAM-2layers) for the YB (a) and UTB (b).

Overall,

Another crucial consideration is whether the information embedded in Lagrangian particles can adequately capture the impact of surface evaporation over the source regions. For example, intense tropical convection continuously lifts lower atmospheric moisture to upper levels and forms precipitation, while strong surface evaporation consistently replenishes moisture to the lower atmosphere. During this process, even though substantial evaporation enters the lower atmosphere, it may not be fully reflected by changes in specific humidity. Additionally, evaporation primarily occurs at the surface, while precipitation moisture condensation mainly happens in the mid-to-upper atmosphere. Therefore, changes in specific humidity in the lower atmosphere may not effectively capture the moisture loss associated with upper-level precipitation. In this context, we randomly selected one trajectory from the SIO leading to precipitation in the YB and another from the NEA responsible for precipitation in the UTB (Fig. S11). Leveraging the high spatial-temporal resolution ERA5 data, we then conducted a comprehensive analysis based on these two trajectories.

Figure 10 illustrates the 6-hourly time series of particle heights (m), 1.5 BLH (m), specific humidity changes (g kg^{-1} 6h^{-1}), vertical velocities in 700 hPa (Pa s^{-1}), precipitation (mm), and evaporation (mm) along the two selected trajectories, with the last three variables extracted from the 0.25°×0.25° and 6-hourly ERA5 dataset. Figure 10 clearly shows the acquisition of moisture in the source regions and subsequent loss upon reaching the target regions (specific humidity changes), pronounced updrafts during monsoonal moisture transport (vertical velocity in Fig. 10a), weak convective activities over the hinterland Eurasia (vertical velocity in Fig. 10b), strong evaporation and precipitation in the ISM-dominated regions (precipitation and evaporation in Fig. 10a), and weak precipitation but strong diurnal evaporation in the westerlies-dominated regions (precipitation and evaporation in Fig. 10b).

We then select six time periods (shaded areas in Fig. 10) for detailed analysis. Relative to Period 1, Period 2 exhibits less moisture loss but stronger convective activities and enhanced precipitation. During period 3, intense atmospheric subsidence is observed, suggesting that evaporation may struggle to transport to the upper atmosphere. Nonetheless, moisture uptake during this period does not show a noticeable reduction. Contrary to Period 4, Period 5 experiences more intense precipitation but is characterized by moisture uptake. During Period 6, minimal evaporation and relatively weak atmospheric subsidence occur, yet the moisture uptake remains comparable to other periods. It should be noted that the comparisons here may involve substantial uncertainties and can be potentially influenced by various meteorological factors. In fact, using specific humidity changes to assess evaporation, precipitation, and moisture transport over source regions still remains challenging. Actually, the "WaterSip" method have already employs a threshold of 1.5 BLH and 0.2 g^{-1} kg^{-1} 6h^{-1} for specific humidity changes to filter out a considerable number of potential erroneous trajectories over the source regions. Specifically, Keune et al. (2022) explored the biases in the "WaterSip" method induced by various threshold settings and introduced an initial framework for diagnosis, attribution, and correction using averaged evaporation and precipitation over the source and sink regions. Ttheis abovethese sensitivity analysesexperiments underscorefurther suggests that the current method approaches of to diagnosing moisture sources around for the TP based usingon particle trajectoriesnumerical moisture tracking models still holds substantial potential for improvement and refinement.

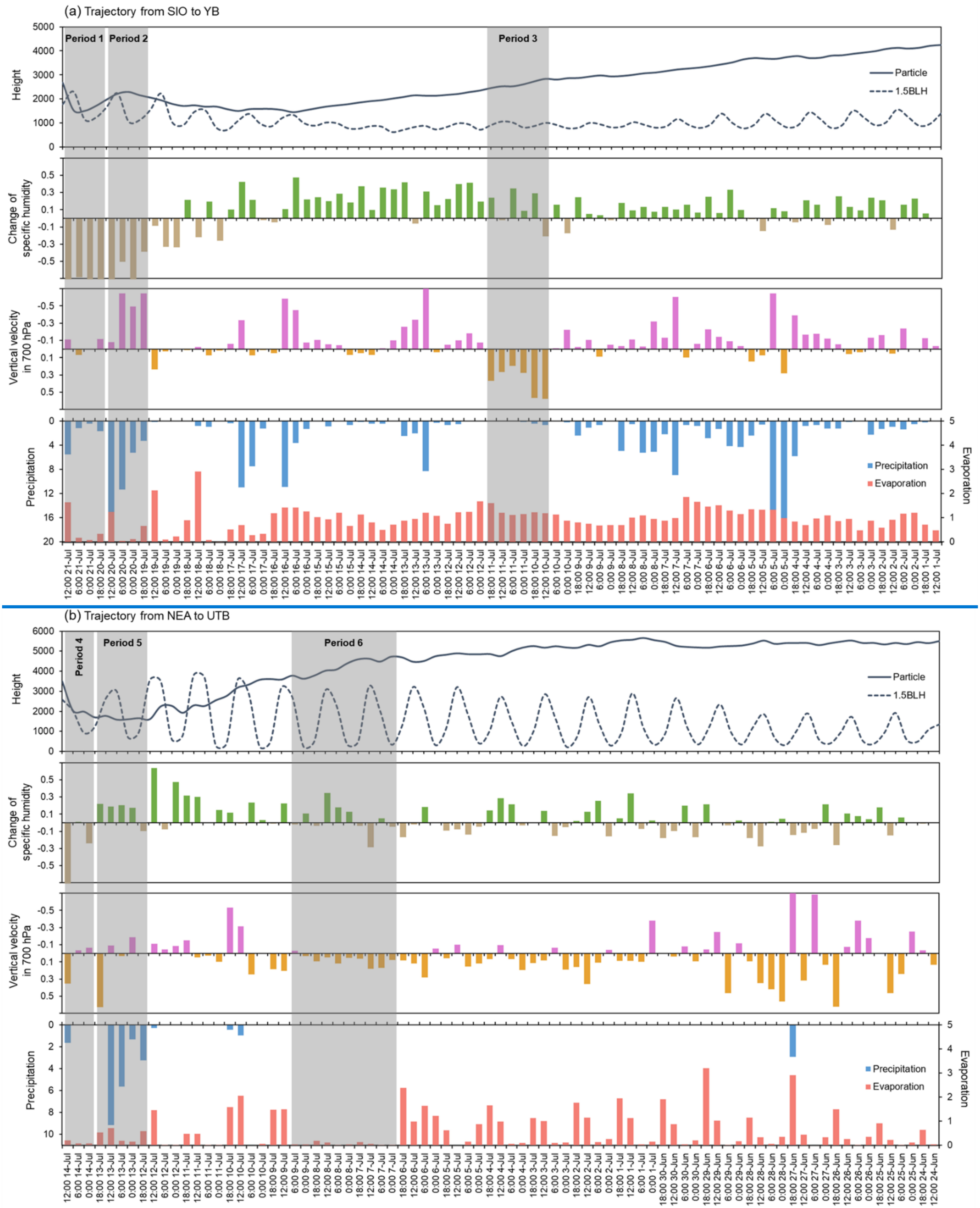
(a) Trajectory from SIO to YB
Period 1
Period 2
Period 3
Height
Particle
1.5BLH
Change of specific humidity
Vertical velocity in 700 hPa
Precipitation
Evaporation
(b) Trajectory from NEA to UTB
Period 4
Period 5
Period 6
Height
Particle
1.5BLH
Change of specific humidity
Vertical velocity in 700 hPa
Precipitation
Evaporation

Figure 10: Time series of particle heights, 1.5 BLH, specific humidity changes, vertical velocities in 700 hPa, precipitation, and evaporation on 6-hourly interval in the selected trajectories from SIO to YB during 12:00 21 July and 12:00 1 July (a) and from NEA to UTB during 12:00 14 July and 12:00 24 June (b). Note that the time series is in reverse order.

6 8 Discussions and conclusions

Over the past few decades, considerable efforts have been directed towardsmade to identifying and quantifying the contributions of moisture sources to precipitation over the TP. A synthesis of these studies reveals indicates that the most commonly used Eulerian and Lagrangian moisture tracking models are WAM-2layers and FLEXPART-WaterSip, respectively. However, the suitability and reliability of these models, which incorporate differing physical mechanisms, for moisture tracking over the TP, especially the potential discrepancies in moisture tracking results, havves not yet been thoroughly examined. To address this gap, this This study addresses this gap by focused focusing on two representative basins surrounding of the TP: the YB (representing the ISM-dominated regions) and the UTB (representing the westerlies-dominated regions). Moisture source contributions to precipitation over these two basins were tracked employing using theboth WAM-2layers and FLEXPART-WaterSip models. We then investigated the differences discrepancies in the moisture tracking results of between these two methods models in the two basins and discussed their potential determinants, through by a series of diagnostic processes including comparisons with actual evaporation, biases correction, and a set of sensitivity experiments..

The WAM-2layers model, designed for moisture tracking based on the water balance equation at a spatial-temporal resolution constrained by the forcing dataset, may faces challenges in accurately capturing moisture transport to target regions through smaller-scale atmospheric phenomenon such as turbulence and convectionprocesses. In comparisonCompared with FLEXPART-WaterSip, the application of WAM-2layers onover the TP is more computationally simpler and more efficient. An persistent issueexisting problem with WAM-2layers, compared torelative to the bias-corrected FLEXPART-WaterSip, is its tendency to estimate higher moisture contributions from the westerlies-dominated sources and distant sources but lower contributions from local recycling and nearby sources downwind of the westerliesopposite to the westerlies direction. However,However, these issuesthis can be mitigated by utilizing a higher spatial- and temporal resolutions for forcing dataset in WAM-2layers (, with a priority should beon improving the temporal resolution), particularly in the ISM-dominated YB region region. In addition, WAM-2layers exhibitoffers one notable advantage over FLEXPART-WaterSip: in that its simulatesd spatial distribution of moisture sources alignsis more consistent more closely with the general pattern of actual evaporation, particularly around the Red Sea and Persian Gulf regions where the surface evaporationcontrast between terrestrial and oceanic disparities between ocean and landevaporation is strong is pronounced., particularly in the YB region.

The FLEXPART model is, designed to track air particles in the atmosphere based on a well-established set of physical mechanisms, is complemented by with the subsequent process of WaterSip method toenables diagnose moisture source- –

receptor ~~processes~~relationships ~~using~~with information from ~~the~~ simulated trajectories. ~~The~~ FLEXPART-WaterSip enables us to investigate the movement of air particles transporting moisture in a ~~more~~ detailed three-dimensional space. We investigated ~~Besides exploring~~ the potential impact of different filtering thresholds in the WaterSip method and varying numbers of released particles ~~release numbers, this work primarily investigates the effects of different filtering thresholds in~~on moisture source~~-~~-receptor ~~process~~ diagnos~~is~~tics ~~within the WaterSip method~~. The simulation of precipitation in the two basins is more sensitive to changes in relative humidity thresholds, ~~whereas~~while adjusting ~~the thresholds of~~ specific humidity change~~s~~ threshold does not ~~result in~~ significantly ~~improvement in simulating~~alter the estimated moisture source contributions. ~~However~~Nevertheless, the ~~nature of~~ WaterSip method facilitates ~~the~~ calibration of simulation biases by comparing results~~them~~ with actual observations (~~i.e.,~~such as precipitation and evaporation). Therefore, ~~in~~if possible~~ conditions permit~~, we recommend bias-correcting the simulations from FLEXPART-WaterSip (~~in addition~~through e.g., ~~to~~ the method ~~provided~~proposed by Keune et al. (2022)~~,~~ or ~~we also introduced a~~the simplified two-step approach proposed in ~~Section 6~~this study). The corrected results ~~significantly~~substantially ~~improve~~ reduce the evaporation biases over the source regions, particularly addressing the ~~issue of evaporative differences~~discrepancies arising from land~~-~~-sea ~~distribution disparities~~contrast in evaporation.

~~Its effectiveness in regions with complex weather conditions is generally inferior to that of FLEXPART-WaterSip when operating with forcing datasets of the same resolution. For instance, over the UTB that is characterized by substantial spatial heterogeneity in local convective activities, WAM-2layers struggles to identify the moisture transported from source regions to the northeast of the basin. Moreover, disparities in simulations between the two models are less pronounced in the ISM-dominated YB compared to the westerlies-dominated UTB. In this context, WAM-2layers, compared to FLEXPART-WaterSip, tend to estimate higher moisture contributions from westerlies-dominated and distant source regions but lower contributions from local and nearby source regions opposite to the westerlies direction. However, these issues can be mitigated by utilizing a higher spatial-temporal resolution forcing dataset in WAM-2layers, particularly in the YB region. This approach helps alleviate the potential overestimation from distant sources and underestimation from local recycling for both basins, although it is less effective in correcting the potential overestimation from nearby westerlies-dominated sources. Despite these challenges, a key advantage of WAM-2layers is its inherent ability to distinguish between moisture from evaporation and precipitation, making it more adept at capturing variations in moisture source contributions arising from different surface evaporation. For instance, in regions surrounding the Red Sea and Persian Gulf regions, FLEXPART-WaterSip primarily detects changes in atmospheric humidity due to intense convection, mainly occurring in the adjacent terrestrial regions, whereas WAM-2layers identifies significantly stronger evaporation from oceans.~~

~~The FLEXPART model is designed to simulate air particles based on a well-established set of physical mechanisms, which enables accurate representation of the three-dimensional movement of particles in the atmosphere. However, the subsequent process of "WaterSip" in diagnosing moisture sources using information from simulated trajectories may potentially introduce additional errors. For instance, matching the information on particles' specific humidity with moisture uptake from evaporation~~

and moisture loss from precipitation is always challenging. Nevertheless, compared to WAM-2layers, FLEXPART-WaterSip offers a precise depiction of the three-dimensional distribution of moisture sources, especially in capturing smaller-scale convective systems with high spatial heterogeneity.

This study provides serves as a valuable reference and guidance for future numerical simulations focusing onaimed at tracking moisture sources in across the TP region, including multiple several crucial aspects such as model selection, the accuracy of forcing data, error and uncertainty evaluationanalysisanalysis, and potential strategies for improving enhancing simulate accuracy. While recognizing that each model is best suited to specific has its most suitable application scenarios, this paper study underscores highlights the importance critical need to account forof considering the inherent differencesdistinct characteristics of between different models and the potential uncertainties in diagnosing moisture tracking resultssource diagnoses. Although this investigationAlthough the current findingsThis work isare limitedconfined to short-term simulations using -WAM-2layers and FLEXPART-WaterSipmodels at a short-term simulations time periodmodels in two typical basins over the TPselected regions. However,, it is anticipated that future research will we look forward to future endeavours that could, on one hand, extend suchis interintercomparisons study to a largerother and more refined spatial-temporal scalesregions and even continental or global scale. On the other handFurthermore, exploringinvestigating the application of the feasibility of employing more advancedsophisticated techniques for moisture source- receptor identification, particularly in improvingthose that enhance the capability of Eulerian or Lagrangian models to capture small-scale atmospheric convection/ and turbulencet processes, would be valuableof significant benefit.

our future work aims to extend to larger and more refined spatial-temporal scales and to explore the feasibility of employing more advanced techniques for moisture source identification in both Eulerian and Lagrangian frameworks.

Code availability. The official website of WAM-2layers is: https://wam2layers.readthedocs.io/en/latest/. The official website of FLEXPART is: https://www.flexpart.eu/. The relevant codes and installation tutorials can be obtained from these official websites. For the WaterSip method, the authoritative website is: https://wiki.app.uib.no/gfi/index.php?title=WaterSip. The WaterSip source code we developed in this study can be foundThe reference Python codes of WaterSip written by ourself is given in Part 3 of the in Supplementary Part 3. All additional algorithmscodes are available on request from the first/corresponding author.

All the original codes are available from these official websites.

Data availability. ERA5 data are publicly available at the Climate Data Store (CDS) (https://cds.climate.copernicus.eu/). The input data of WAM-2layers waswere downloaded according to the example code in https://github.com/WAM2layers/WAM2layers/tree/main/scripts. The forcing data of FLEXPART waswere downloaded and pre-processed using the flex_extract v7.1.2 (https://www.flexpart.eu/flex_extract/). All simulation results in this study are available on request from the first/corresponding author.

Author contributions. YL conceptualized the study, carried out numerical simulations, conducted formal analysis, prepared figures, and wrote the initial draft. CW contributed to the editing, discussion, and interpretation. QT, SY, and BS provided comments on the manuscript. HP and SX provided supervision during the simulations and writing.

Competing interests. The contact author has declared that neither they nor their co-authors have any competing interests.

Acknowledgements. We thank Ruud van der Ent and Harald Sodemann for their invaluable and constructive ~~providing excellent guidance~~feedback ~~during the review of~~on earlier versions of this ~~paper~~manuscript. We also thank~~, and~~ the editor for their ~~timely~~efficient handling and insightful feedback throughout the review process.

Financial support. This work was financially supported by the Second Tibetan Plateau Scientific Expedition and Research Program (grant no. 2019QZKK0207-02) and the Natural Science Foundation of Hubei Province of China (grant no. 2022CFB785).

References

!!! INVALID CITATION !!! (van der Ent et al., 2014; Link et al., 2020)

!!! INVALID CITATION !!! (Wang et al., 2018; Tuinenburg and Staal, 2020)

Ayantobo, O.O., Wei, J., Hou, M., Xu, J., Wang, G.: Characterizing potential sources and transport pathways of intense moisture during extreme precipitation events over the Tibetan Plateau, J. Hydrol. 615, 128734, https://doi.org/10.1016/j.jhydrol.2022.128734, 2022

Chen, B., Xu, X.D., Yang, S., Zhang, W.: On the origin and destination of atmospheric moisture and air mass over the Tibetan Plateau, Theor. Appl. Climatol. 110, 423-435, https://doi.org/10.1007/s00704-012-0641-y, 2012

Chen, B., Zhang, W., Yang, S., Xu, X.D.: Identifying and contrasting the sources of the water vapor reaching the subregions of the Tibetan Plateau during the wet season, Climate Dyn. 53, 6891-6907, https://doi.org/10.1007/s00382-019-04963-2, 2019

Chen, Y., Liu, B., Cai, X., Zhou, T., He, Q.: Moisture transport and sources of an extreme rainfall event of June 2021 in southern Xinjiang, China, Adv. Clim. Change Res. 13, 843-850, https://doi.org/10.1016/j.accre.2022.11.010, 2022

Cloux, S., Garaboa-Paz, D., Insua-Costa, D., Miguez-Macho, G., Pérez-Muñuzuri, V.: Extreme precipitation events in the Mediterranean area: contrasting two different models for moisture source identification, Hydrol. Earth Syst. Sci. 25, 6465-6477, https://doi.org/10.5194/hess-25-6465-2021, 2021

Curio, J., Scherer, D.: Seasonality and spatial variability of dynamic precipitation controls on the Tibetan Plateau, Earth Syst. Dynam. 7, 767-782, https://doi.org/10.5194/esd-7-767-2016, 2016

Fremme, A., Sodemann, H.: The role of land and ocean evaporation on the variability of precipitation in the Yangtze River valley, Hydrol. Earth Syst. Sci. 23, 2525-2540, https://doi.org/10.5194/hess-23-2525-2019, 2019

Gimeno, L., Stohl, A., Trigo, R.M., Dominguez, F., Yoshimura, K., Yu, L., Drumond, A., Durán-Quesada, A.M., Nieto, R.: Oceanic and terrestrial sources of continental precipitation, Rev. Geophys. 50, RG4003, https://doi.org/10.1029/2012RG000389, 2012

Gimeno, L., Vazquez, M., Eiras-Barca, J., Sori, R., Stojanovic, M., Algarra, I., Nieto, R., Ramos, A.M., Duran-Quesada, A.M., Dominguez, F.: Recent progress on the sources of continental precipitation as revealed by moisture transport analysis, Earth-Sci. Rev. 201, 103070, https://doi.org/10.1016/j.earscirev.2019.103070, 2020

Guo, L., van der Ent, R.J., Klingaman, N.P., Demory, M.-E., Vidale, P.L., Turner, A.G., Stephan, C.C., Chevuturi, A.: Moisture Sources for East Asian Precipitation: Mean Seasonal Cycle and Interannual Variability, J. Hydrometeorol. 20, 657-672, https://doi.org/10.1175/JHM-D-18-0188.1, 2019

Guo, L., van der Ent, R.J., Klingaman, N.P., Demory, M.E., Vidale, P.L., Turner, A.G., Stephan, C.C., Chevuturi, A.: Effects of horizontal resolution and air–sea coupling on simulated moisture source for East Asian precipitation in MetUM GA6/GC2, Geosci. Model Dev. 13, 6011-6028, https://doi.org/10.5194/gmd-13-6011-2020, 2020

Hersbach, H., Bell, B., Berrisford, P., Hirahara, S., Horanyi, A., Munoz-Sabater, J., Nicolas, J., Peubey, C., Radu, R., Schepers, D., Simmons, A., Soci, C., Abdalla, S., Abellan, X., Balsamo, G., Bechtold, P., Biavati, G., Bidlot, J., Bonavita, M., De Chiara, G., Dahlgren, P., Dee, D., Diamantakis, M., Dragani, R., Flemming, J., Forbes, R., Fuentes, M., Geer, A., Haimberger, L., Healy, S., Hogan, R.J., Holm, E., Janiskova, M., Keeley, S., Laloyaux, P., Lopez, P., Lupu, C., Radnoti, G., de Rosnay, P., Rozum, I., Vamborg, F., Villaume, S., Thepaut, J.-N.: The ERA5 global reanalysis, Quart. J. Roy. Meteorol. Soc. 146, 1999-2049, https://doi.org/10.1002/qj.3803, 2020

Hu, Q., Zhao, Y., Huang, A., Ma, P., Ming, J.: Moisture Transport and Sources of the Extreme Precipitation Over Northern and Southern Xinjiang in the Summer Half-Year During 1979–2018, Frontiers in Earth Science 9, https://doi.org/10.3389/feart.2021.770877, 2021

Huang, W., Qiu, T., Yang, Z., Lin, D., Wright, J.S., Wang, B., He, X.: On the formation mechanism for wintertime extreme precipitation events over the southeastern Tibetan Plateau, J. Geophys. Res.-Atmos. 123, 12,692-612,714, https://doi.org/10.1029/2018JD028921, 2018

Keune, J., Schumacher, D.L., Miralles, D.G.: A unified framework to estimate the origins of atmospheric moisture and heat using Lagrangian models, Geosci. Model Dev. 15, 1875-1898, https://doi.org/10.5194/gmd-15-1875-2022, 2022

Li, Y., Su, F., Chen, D., Tang, Q.: Atmospheric Water Transport to the Endorheic Tibetan Plateau and Its Effect on the Hydrological Status in the Region, J. Geophys. Res.-Atmos. 124, 12864-12881, https://doi.org/10.1029/2019jd031297, 2019

Li, Y., Su, F., Tang, Q., Gao, H., Yan, D., Peng, H., Xiao, S.: Contributions of moisture sources to precipitation in the major drainage basins in the Tibetan Plateau, Sci. China-Earth Sci. 65, 1088, https://doi.org/10.1007/s11430-021-9890-6, 2022a

Li, Y., Wang, C., Huang, R., Yan, D., Peng, H., Xiao, S.: Spatial distribution of oceanic moisture contributions to precipitation over the Tibetan Plateau, Hydrol. Earth Syst. Sci. 26, 6413-6426, https://doi.org/10.5194/hess-26-6413-2022, 2022b

Liu, R., Wang, X., Wang, Z.: Atmospheric moisture sources of drought and wet events during 1979–2019 in the Three-River Source Region, Qinghai-Tibetan Plateau, Theor. Appl. Climatol. 149, 487-499, https://doi.org/10.1007/s00704-022-04058-9, 2022

Liu, R., Wen, J., Wang, X., Wang, Z., Liu, Y.: Case studies of atmospheric moisture sources in the source region of the Yellow River from a Lagrangian perspective, Int. J. Climatol. 42, 1516-1530, https://doi.org/10.1002/joc.7317, 2021

Liu, X., Liu, Y., Wang, X., Wu, G.: Large-Scale Dynamics and Moisture Sources of the Precipitation Over the Western Tibetan Plateau in Boreal Winter, J. Geophys. Res.-Atmos. 125, e2019JD032133, https://doi.org/10.1029/2019JD032133, 2020a

Liu, Y., Lu, M., Yang, H., Duan, A., He, B., Yang, S., Wu, G.: Land–atmosphere–ocean coupling associated with the Tibetan Plateau and its climate impacts, Natl. Sci. Rev. 7, 534-552, https://doi.org/10.1093/nsr/nwaa011, 2020b

Ma, Y., Lu, M., Bracken, C., Chen, H.: Spatially coherent clusters of summer precipitation extremes in the Tibetan Plateau: Where is the moisture from?, Atmos. Res. 237, 104841, https://doi.org/10.1016/j.atmosres.2020.104841, 2020

Pan, C., Zhu, B., Gao, J., Kang, H., Zhu, T.: Quantitative identification of moisture sources over the Tibetan Plateau and the relationship between thermal forcing and moisture transport, Climate Dyn. 52, 181-196, https://doi.org/10.1007/s00382-018-4130-6, 2018

Pisso, I., Sollum, E., Grythe, H., Kristiansen, N.I., Cassiani, M., Eckhardt, S., Arnold, D., Morton, D., Thompson, R.L., Groot Zwaaftink, C.D., Evangeliou, N., Sodemann, H., Haimberger, L., Henne, S., Brunner, D., Burkhart, J.F., Fouilloux, A., Brioude, J., Philipp, A., Seibert, P., Stohl, A.: The Lagrangian particle dispersion model FLEXPART version 10.4, Geosci. Model Dev. 12, 4955-4997, https://doi.org/10.5194/gmd-12-4955-2019, 2019

Qiu, T., Huang, W., Wright, J.S., Lin, Y., Lu, P., He, X., Yang, Z., Dong, W., Lu, H., Wang, B.: Moisture Sources for Wintertime Intense Precipitation Events Over the Three Snowy Subregions of the Tibetan Plateau, J. Geophys. Res.-Atmos. 124, 12708-12725, https://doi.org/10.1029/2019jd031110, 2019

Shao, L., Tian, L., Cai, Z., Wang, C., Li, Y.: Large-scale atmospheric circulation influences the ice core d-excess record from the central Tibetan Plateau, Climate Dyn. 57, 1805-1816, https://doi.org/10.1007/s00382-021-05779-9, 2021

Sodemann, H., Schwierz, C., Wernli, H.: Interannual variability of Greenland winter precipitation sources: Lagrangian moisture diagnostic and North Atlantic Oscillation influence, J. Geophys. Res.-Atmos. 113, D03107, https://doi.org/10.1029/2007JD008503, 2008

Sprenger, M., Wernli, H.: The LAGRANTO Lagrangian analysis tool – version 2.0, Geosci. Model Dev. 8, 2569-2586, https://doi.org/10.5194/gmd-8-2569-2015, 2015

Stein, A.F., Draxler, R.R., Rolph, G.D., Stunder, B.J.B., Cohen, M.D., Ngan, F.: NOAA's HYSPLIT Atmospheric Transport and Dispersion Modeling System, Bull. Amer. Meteorol. Soc. 96, 2059-2078, https://doi.org/10.1175/BAMS-D-14-00110.1, 2016

Sun, B., Wang, H.: Moisture sources of semiarid grassland in China using the Lagrangian particle model FLEXPART, J. Climate 27, 2457-2474, https://doi.org/10.1175/JCLI-D-13-00517.1, 2014

Tuinenburg, O.A., Staal, A.: Tracking the global flows of atmospheric moisture and associated uncertainties, Hydrol. Earth Syst. Sci. 24, 2419-2435, https://doi.org/10.5194/hess-24-2419-2020, 2020

van der Ent, R.J., Savenije, H.H., Schaefli, B., Steele-Dunne, S.C.: Origin and fate of atmospheric moisture over continents, Water Resour. Res. 46, W09525, https://doi.org/10.1029/2010WR009127, 2010

van der Ent, R.J., Tuinenburg, O.A., Knoche, H.R., Kunstmann, H., Savenije, H.H.G.: Should we use a simple or complex model for moisture recycling and atmospheric moisture tracking?, Hydrol. Earth Syst. Sci. 17, 4869-4884, https://doi.org/10.5194/hess-17-4869-2013, 2013

van der Ent, R.J., Wang-Erlandsson, L., Keys, P.W., Savenije, H.H.G.: Contrasting roles of interception and transpiration in the hydrological cycle – Part 2: Moisture recycling, Earth Syst. Dynam. 5, 471-489, https://doi.org/10.5194/esd-5-471-2014, 2014

Wang, L., Liu, W., Xu, Z., Zhang, J.: Water sources and recharge mechanisms of the Yarlung Zangbo River in the Tibetan Plateau: Constraints from hydrogen and oxygen stable isotopes, J. Hydrol. 614, 128585, https://doi.org/10.1016/j.jhydrol.2022.128585, 2022

Wang, Y., Yang, K., Huang, W., Qiu, T., Wang, B.: Dominant Contribution of South Asia Monsoon to External Moisture for Extreme Precipitation Events in Northern Tibetan Plateau, Remote Sensing 15, 735, https://doi.org/10.3390/rs15030735, 2023

Winschall, A., Pfahl, S., Sodemann, H., Wernli, H.: Comparison of Eulerian and Lagrangian moisture source diagnostics – the flood event in eastern Europe in May 2010, Atmos. Chem. Phys. 14, 6605-6619, https://doi.org/10.5194/acp-14-6605-2014, 2014

Xu, Y., Gao, Y.: Quantification of Evaporative Sources of Precipitation and Its Changes in the Southeastern Tibetan Plateau and Middle Yangtze River Basin, Atmosphere 10, 428, https://doi.org/10.3390/atmos10080428, 2019

Yang, K., Wu, H., Qin, J., Lin, C., Tang, W., Chen, Y.: Recent climate changes over the Tibetan Plateau and their impacts on energy and water cycle: A review, Glob. Planet. Change 112, 79-91, https://doi.org/10.1016/j.gloplacha.2013.12.001, 2014

Yang, S., Zhang, W., Chen, B., Xu, X., Zhao, R.: Remote moisture sources for 6-hour summer precipitation over the Southeastern Tibetan Plateau and its effects on precipitation intensity, Atmos. Res. 236, 104803, https://doi.org/10.1016/j.atmosres.2019.104803, 2020

Yao, S., Jiang, D., Zhang, Z.: Lagrangian simulations of moisture sources for Chinese Xinjiang precipitation during 1979–2018, Int. J. Climatol. 41, E216-E232, https://doi.org/10.1002/joc.6679, 2020

Yao, S., Jiang, D., Zhang, Z.: Moisture Sources of Heavy Precipitation in Xinjiang Characterized by Meteorological Patterns, J. Hydrometeorol. 22, 2213-2225, https://doi.org/10.1175/JHM-D-20-0236.1, 2021

Yao, T., Bolch, T., Chen, D., Gao, J., Immerzeel, W., Piao, S., Su, F., Thompson, L., Wada, Y., Wang, L., Wang, T., Wu, G., Xu, B., Yang, W., Zhang, G., Zhao, P.: The imbalance of the Asian water tower, Nature Reviews Earth & Environment https://doi.org/10.1038/s43017-022-00299-4, 2022

Yao, T., Masson-Delmotte, V., Gao, J., Yu, W., Yang, X., Risi, C., Sturm, C., Werner, M., Zhao, H., He, Y.: A review of climatic controls on δ18O in precipitation over the Tibetan Plateau: Observations and simulations, Rev. Geophys. 51, 525-548, https://doi.org/10.1002/rog.20023, 2013

Yao, T., Xue, Y., Chen, D., Chen, F., Thompson, L., Cui, P., Koike, T., Lau, W.K.-M., Lettenmaier, D., Mosbrugger, V.: Recent Third Pole's rapid warming accompanies cryospheric melt and water cycle intensification and interactions between monsoon and environment: multi-disciplinary approach with observation, modeling and analysis, Bull. Amer. Meteorol. Soc. 100, 423-444, https://doi.org/10.1175/BAMS-D-17-0057.1, 2018

Zhang, C.: Moisture source assessment and the varying characteristics for the Tibetan Plateau precipitation using TRMM, Environ. Res. Lett. 15, 104003, https://doi.org/10.1088/1748-9326/abac78, 2020

Zhang, C., Chen, D., Tang, Q., Huang, J.: Fate and Changes in Moisture Evaporated From the Tibetan Plateau (2000–2020), Water Resour. Res. 59, e2022WR034165, https://doi.org/10.1029/2022WR034165, 2023a

Zhang, C., Tang, Q., Chen, D.: Recent changes in the moisture source of precipitation over the Tibetan Plateau, J. Climate 30, 1807-1819, https://doi.org/10.1175/JCLI-D-15-0842.1, 2017

Zhang, C., Tang, Q.H., Chen, D.L., van der Ent, R.J., Liu, X.C., Li, W.H., Haile, G.G.: Moisture Source Changes Contributed to Different Precipitation Changes over the Northern and Southern Tibetan Plateau, J. Hydrometeorol. 20, 217-229, https://doi.org/10.1175/Jhm-D-18-0094.1, 2019a

Zhang, C., Zhang, X., Tang, Q., Chen, D., Huang, J., Wu, S., Liu, Y.: Quantifying precipitation moisture contributed by different atmospheric circulations across the Tibetan Plateau, J. Hydrol. 628, 130517, https://doi.org/10.1016/j.jhydrol.2023.130517, 2024

Zhang, Q., Shen, Z., Pokhrel, Y., Farinotti, D., Singh, V.P., Xu, C., Wu, W., Wang, G.: Oceanic climate changes threaten the sustainability of Asia's water tower, Nature 615, 87-93, https://doi.org/10.1038/s41586-022-05643-8, 2023b

Zhang, Y., Huang, W., Zhong, D.: Major Moisture Pathways and Their Importance to Rainy Season Precipitation over the Sanjiangyuan Region of the Tibetan Plateau, J. Climate 32, 6837-6857, https://doi.org/10.1175/jcli-d-19-0196.1, 2019b

Zhao, R., Chen, B., Xu, X.: Intensified Moisture Sources of Heavy Precipitation Events Contributed to Interannual Trend in Precipitation Over the Three-Rivers-Headwater Region in China, Frontiers in Earth Science 9, https://doi.org/10.3389/feart.2021.674037, 2021

Zhao, R., Chen, B., Zhang, W., Yang, S., Xu, X.: Moisture source anomalies connected to flood-drought changes over the three-rivers headwater region of Tibetan Plateau, Int. J. Climatol. 43, 5303-5316, https://doi.org/10.1002/joc.8147, 2023

Zhou, Y., Xie, Z., Liu, X.: An Analysis of Moisture Sources of Torrential Rainfall Events over Xinjiang, China, J. Hydrometeorol. 20, 2109-2122, https://doi.org/10.1175/JHM-D-19-0010.1, 2019